2020

The role of behavioral diversity in determining the extent to which central pattern generators are modulated

Jacob Salman Kazmi
Bowdoin College

The role of behavioral diversity in determining the extent to which central pattern generators are modulated

An Honors Project for the Program of Neuroscience

By Jacob Salman Kazmi

Bowdoin College, 2020

TABLE OF CONTENTS

ACKNOWLEDGEMENTS

This project could not have been completed without the unwavering support of my advisor, Patsy Dickinson. Thank you, Patsy, for always offering help and guidance to me and the other members of the lab. Her dedication to not only neuroscience research, but to teaching and mentorship has impacted all of us. She has shown me the joy and excitement of research, as well as the constant balancing act of a researcher's life. My almost four years in the Dickinson Lab have taught me many skills and values, all of which I am very grateful for. Additionally, I would like to thank all faculty members of the Neuroscience Program at Bowdoin College, particularly my thesis reviewers Erika Nyhus and Hadley Horch. Thank you for your efforts in bringing a liberal arts mindset to a STEM curriculum in a unique and meaningful way.

The transcriptomics portion of this project was greatly supported by Andy Christie at the University of Hawaii at Manoa and Joel Graber at the Mount Desert Island Biological Laboratory. Andy taught me the basics of bioinformatics a couple of years ago, sparking an interest that led to the inclusion of these analyses in this project. Thank you, Joel for your help in constructing these methods, making sense of these results, and teaching me how to bring context to a bioinformatics workflow.

Thank you to the past and present members of the Dickinson Lab. I adopted this project from Ali Miller after her graduation in 2018. She was a great mentor and inspired me to continue her work for my honors project. Ricky Tsang was a great teacher as well, and he taught me the long and arduous STNS dissections. Without his help and support, I would not have been able to complete any of these dissections. Grace Bukowski-Thall was my collaborator on this project, and although we hit many bumps with this project along the way, I am proud to say that we

completed it. I hope that my assistant on this project, Kenny Garcia, to whom I am very grateful for his help in running my physiological experiments, will continue this work in the future.

In order to obtain the snow crabs used in this study, Audrey Jordan, Nate Blum, and Ben Wong accompanied me on the long trip to Halifax, Nova Scotia. I am indebted to all of you for joining me, and I will remember that great trip for a long time. Of course, a big thank you to Marko Melendy and the animal caretakers at Bowdoin College. Marko and his team ensure the health and care of all of our animals, and his work is greatly appreciated.

To my parents, Galina Bass and Mehdi Kazmi, thank you for giving me the confidence to pursue such an endeavor. By sending me to Bowdoin, know that the values that you have instilled in me from a young age have been strengthened and fostered. Thank you to Micki Lee Coleman-Palansky for supporting me through all four years of college, and for listening to my constant ramblings on science. To my roommates and friends at Bowdoin, I am sorry that our senior year was cut short, but I thank you for coming to visit me in the lab, listening to my practice talks, and helping me keep my sanity throughout my time at Bowdoin. I am sad that we won't be able to see each other for graduation, but I am looking forward to seeing you all very soon.

This research project was supported by the Bowdoin College Neuroscience Program, the Paller Neuroscience Research Fellowship, the Henry L. and Grace Doherty Charitable Foundation Coastal Studies Research Fellowship, the National Institutes of Health through a Maine INBRE Summer Research Fellowship [P20GM103423], and the National Science Foundation [IOS-1354567 to Patsy Dickinson].

ABSTRACT

Neuromodulation may be a substrate for the evolution of behavioral diversity. In the case of central pattern generators, the extent to which a pattern is modulated could serve as a mechanism that enables variability in motor output dependent on an organism's need for behavioral flexibility. The pyloric circuit is one of four central pattern generators in the crustacean stomatogastric nervous system (STNS); its outputs stimulate contractions of foregut muscles in digestion. The sensitivity of the pyloric circuit to various neuromodulatory molecules has been examined in two crab species. One of these species, *Cancer borealis*, is an opportunistic feeder, while the other, *Pugettia producta,* is a specialist feeder subsisting on kelp. Since neuromodulation enables variation in the movements of pyloric muscles, without altering STNS circuitry, more diverse feeding patterns should be correlated with a higher degree of STNS neuromodulation. Previous data have shown that *C. borealis* is sensitive to a wider array of neuromodulators than *P. producta,* which could be a result of behavioral diversity. The observed difference in modulatory capacity may, however, be coincidental since these species are separated by phylogeny. Preliminary data show that *Libinia emarginata*, a member of the same superfamily as *P. producta*, is sensitive to the same neuromodulators as *C. borealis*, negating phylogenetic distance as the major contributing factor to the observed array of neuromodulation (Miller, 2018). We predict that the difference in modulatory capacity is a product of a differential need for variety in foregut muscle movement patterns while digesting. In an attempt to further elucidate the relationships between diet, phylogeny, and stomatogastric modulation, this study examined a member of the same superfamily as *P. producta,* the opportunistic-feeding snow crab (*Chionoecetes opilio*). Using extracellular recording methods, the responses of isolated STNS preparations to six endogenous neuromodulators and an

acetylcholine receptor agonist were measured. Bursting parameters were analyzed to determine whether each neuromodulator affected the pyloric pattern. Initial qualitative results indicate that the STNS of *C. opilio* is sensitive to all of these neuromodulators. Further physiological experiments are needed to determine the neuromodulatory capacity of this organism. Additionally, previous data on the neuromodulatory capacity of *L. emarginata* was supported through similar electrophysiological analysis of the isolated STNS. As a first step in determining the mechanism of differential sensitivity between species, tissue-specific transcriptomes were generated and mined for neuromodulators.

INTRODUCTION

An organism's nervous system must be flexible in order to cope with various changes in the environment that may be present throughout its lifespan. The nervous system is able to alter and control behavior and neuronal function, on small timescales, through neuromodulation. Neuromodulators, endogenous molecules that alter neuronal firing patterns, are crucial in enabling behavioral diversity and possibly behavioral evolution. For example, the neuromodulator serotonin lowers the threshold for non-associative sensitization in the California sea hare, *Aplysia californica* (Hoover et al., 2006). Neuromodulators enable a single neuronal circuit to produce a diverse set of behaviors in both a single species and closely related organisms through evolutionarily conserved mechanisms (Katz and Harris-Warrick, 1999). The neuromodulators employed by closely related organisms are known to vary, and behaviors vary accordingly. Notably, in three related species of the Aplysiidae family, differing sensitivity to touch has been correlated with differing responses to neuromodulators (Hoover et al., 2006). Developments in the study of neuromodulatory networks raise three critical questions, which this study seeks to address: Is the modulatory capacity, or the extent to which a circuit is modulated, of a single organism a mechanism that underlies the system's behavioral diversity? Is the variability in the degree of neuromodulation between closely related organisms a result of phylogenetic distance or ecological need (e.g. available food sources)? What are the mechanisms of evolution-scale changes in modulatory capacity?

Central pattern generators (CPGs) are relatively simple, multi-functional networks that produce rhythmic motor outputs independent of sensory input (reviewed in Marder and Bucher, 2001). CPGs drive various rhythmic behaviors such as breathing, digestion, and locomotion. Neuromodulators are known to act on these CPGs, in both vertebrates and invertebrates, altering

rhythmic outputs and facilitating interactions between CPGs (Dickinson, 2006). As a result, a variety of behaviors can arise from a single CPG circuit.

The decapod crustacean stomatogastric nervous system (STNS) contains four distinct CPGs, each controlling a different section of the foregut. The stomatogastric ganglion (STG) is a crucial part of this system and is highly conserved throughout the order Decapoda (Katz and Harris-Warrick, 1999). *In vivo*, STG outputs innervate muscles, while *in vitro*, isolated STGs still produce highly patterned and detectable outputs (Marder and Bucher, 2001). Therefore, the isolated STG is a suitable model for studying the effects of neuromodulatory molecules on target circuits.

The roughly 30 neurons within the STG comprise two different CPGs within the foregut, producing the gastric mill pattern and the pyloric pattern (reviewed in Daur et al., 2016). The gastric mill pattern is responsible for tooth movements within the gastric mill, and is generally considered to have a relatively slow timescale (Selverston et al., 2009). The STG is also responsible for neural control of the pylorus, which is involved in the moving and filtering of food particles into the midgut, via the faster pyloric pattern (Harris-Warrick, 1989).

The core pyloric pattern consists of a triphasic rhythm caused by the consecutive firing of the Pyloric Dilator (PD), Lateral Pyloric (LP), and Pyloric (PY) neurons. Additional bursting from the Inferior Cardiac (IC) and the Ventricular Dilator (VD) neurons supplements the core pattern. The somata and dendrites of these cells, which house neuromodulator receptors, are contained within the STG. The projections of these five different neuron types innervate different muscle groups, which allow the pylorus to pass food down the digestive tract. The musculature of the pylorus and its neuronal control have been well characterized in the American lobster (*Homarus* americanus) through electromyographic and endoscopic studies. PD neurons innervate

the muscles of the cardio-pyloric valve, which forms a sphincter and limits the size of food particles that pass from the gastric mill into the pylorus (Govind and Lingle, 1987). LP neurons innervate another set of intrinsic cardio-pyloric valve muscles that move food particles into the main chamber of the pylorus. PY neurons innervate the prominent pyloric intrinsic muscle 1, which upon contraction assists in passing food through the chamber of the pylorus (Maynard and Dando, 1974). These three motoneurons work together in a relatively simple circuit to allow phasic behavioral outputs.

The core rhythm is a product of the intrinsic neuronal properties of each neuron type and the inhibitory synapses that connect them (Fig. 1). The pattern is driven by rhythmic activity of the intrinsically oscillating anterior burster (AB) neuron, which is electrotonically coupled to PD neurons (Marder and Eisen, 1984). AB and PD operate in tandem to inhibit LP and PY neurons. Due to inherent physiological properties, LP neurons quickly rebound and fire, which further inhibits PY neurons. PY neurons exhibit a delayed post-inhibitory rebound, and in turn inhibit LP neuron firing to end the LP phase (reviewed in Marder and Bucher, 2007). This cycle of rebound inhibition driven by AB and PD gives rise to the triphasic characteristic of the pyloric pattern. Neuromodulators alter the physiological characteristics and firing behaviors of these neurons to modify the pyloric pattern.

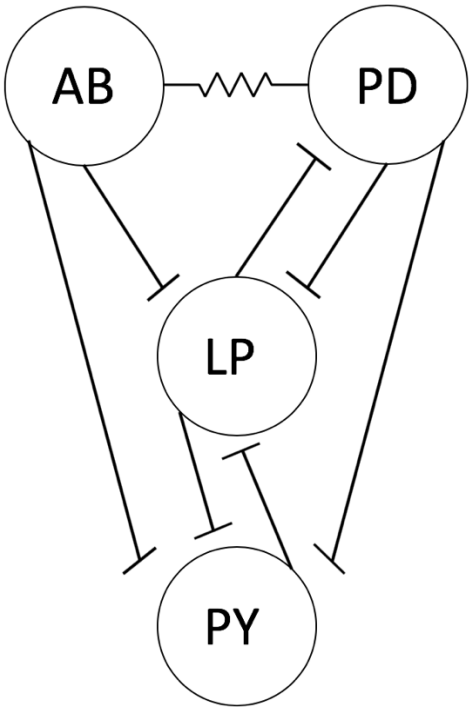

Figure 1. A simplified depiction of the pyloric circuit. The intrinsic oscillator neuron AB drives the pyloric rhythm and is electrotonically coupled to PD neurons. The three motor neurons PD, LP, and PY inhibit each other giving rise to the triphasic core pyloric pattern. Each circle represents a neuron type, the resistor symbol represents electrotonic coupling, and t-shaped lines signify inhibitory synapses. Adapted from (Marder and Bucher, 2007)

As a central pattern, the pyloric pattern is modulated, in a way that is dependent on the organism's feeding state, by endogenous neuropeptides and neurohormones (reviewed in Harris-Warrick, 1989). These modulatory signaling molecules allow for short timescale behavioral adaptations. Dopamine is one such compound, and has been shown to increase hyperpolarization-activated inward cation currents in AB neurons to increase bursting frequency (Peck et al., 2006). Functionally, this increases the rate of the pyloric pattern and allows the pyloric muscles to contract more frequently for faster filtering of food particles (Kadiri et al., 2011). *In vivo*, the pyloric circuit receives modulatory inputs from a variety of secretory tissues. Some of these modulatory molecules are released into the animal's circulatory fluid, or hemolymph, and likely have multiple targets. For example, cholecystokinin-like peptide is

released by brain, eyestalk, and commissural ganglia tissues and has been shown to have direct effects on the pyloric rhythm (Turrigiano and Selverston, 1989). Other modulatory inputs come from neurons that synapse directly onto STG neurons, such as the anterior pyloric modulator neuron in the oesophageal ganglion (Dickinson and Nagy, 1983). The behavioral action of modulators is not surprising, as circuits must be flexible to adapt to environmental pressures such as changes in feeding state.

Diets of decapod crustacean species can vary, with some members being specialist feeders and others opportunistic feeders. Opportunistic feeders, with diverse food sources, require manifold gastric movements to digest different foods. In contrast, specialist feeders subsist on a single or a few related food sources, and likely do not require as varied gastric movements. Since neuromodulation enables variations in movements of foregut musculature, without altering STNS circuitry, diversity of feeding patterns should be indicative of the degree of STNS neuromodulation, dubbed neuromodulatory capacity.

The herbivorous crab *Pugettia producta*, a member of the Majoidea superfamily, shows a lower degree of modulation by endogenous neuropeptides than an opportunistic feeder in the Cancroidea superfamily, *Cancer borealis* (Dickinson et al., 2008). However, given that these two species belong to different superfamilies, the observed differences in neuromodulatory capacity may be a product of phylogenetic distance. Evaluating the neuromodulatory capacity of related Majoid crabs can control for the possible effects of phylogeny. Recent data from a similar STNS neuromodulatory study of *Libinia emarginata*, an opportunistic feeder that belongs to the Majoidea superfamily, shows that the *Libinia* STNS is indeed affected by more neuromodulators than the *Pugettia* STNS (Miller, 2018). This suggests that differential modulation is a result of diet diversity, rather than phylogenetic distance, as these species are closely related.

This study continues investigating the relationship between neuromodulation and evolutionary pressures by examining the above theories in an organism that has never been the subject of nervous system study, the snow crab (*Chionoecetes opilio*). *C. opilio* is an opportunistically feeding member of the superfamily Majoidea and is native to the northwest Atlantic and northern Pacific Oceans (Sainte-Marie et al., 1997). Although it is also a member of the Majoidea superfamily, *C. opilio* is somewhat more distantly related to *P. producta* than *L. emarginata* is to *P. producta* (Fig. 2) (Hultgren and Stachowicz, 2008). Examining the correlation between the range of neuromodulators functioning in the STNS of *C. opilio* and its status as an opportunistic feeder will further explain the relationships between diet, stomatogastric neuromodulation, and phylogeny.

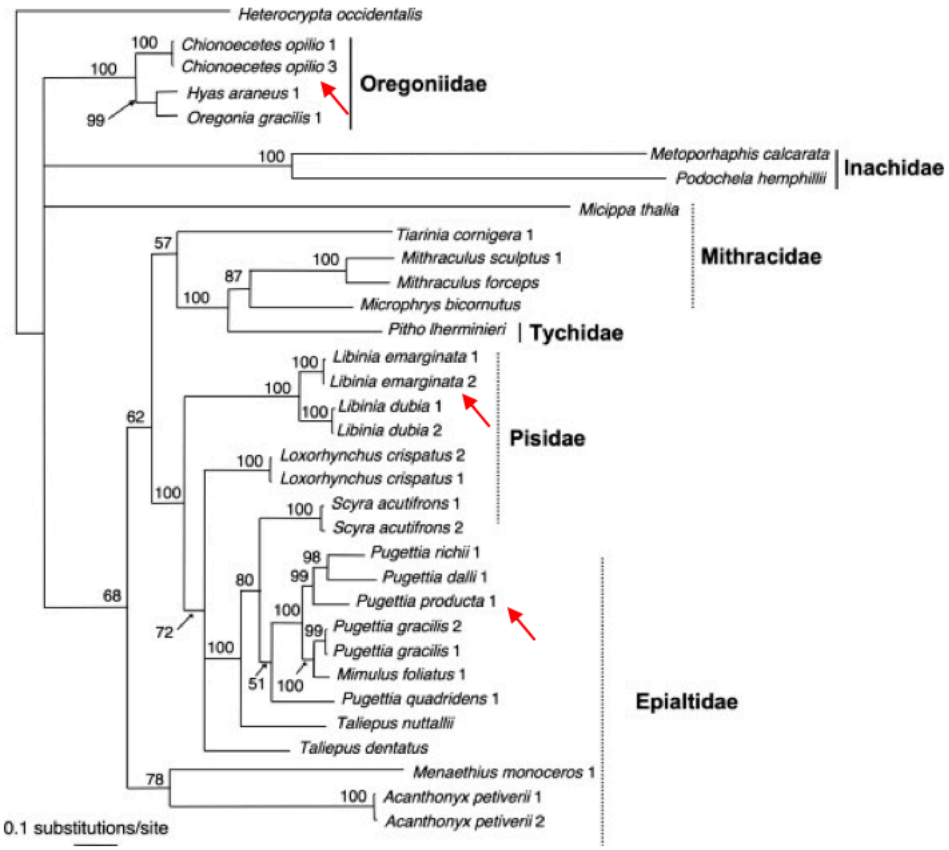

Figure 2. Phylogenetic tree of the Majoidea superfamily generated from genetic data. The distance between *C. opilio* and *P. producta* is greater than the distance between *L. emarginata* and *P. producta*. Numbers represent slight intraspecies genetic variations, arrows indicate species of interest. Adapted from (Hultgren and Stachowicz, 2008).

Given that *C. opilio* is an opportunistic feeder, it is hypothesized that *C. opilio* has a neuromodulatory capacity similar to that of *L. emarginata*, another opportunistic feeder. Thus, we also predict that the STNS of *C. opilio* will be sensitive to a wider variety of neuromodulators, i.e. have a broader neuromodulatory capacity, than the specialist feeder *P. producta*.

Extracellular recordings of the pyloric pattern in isolated STNS preparations allow for a quantified evaluation of neuromodulator sensitivity in *C. opilio*, which can be compared to the respective neuromodulator sensitivities of *L. emarginata* and *P. producta*. Seven neuromodulators, all of which have been shown to be highly conserved within decapod

crustacean species, were applied to the STNS of *C. opilio* (Dickinson et al., 2008). All seven of these modulators elicit changes in the pyloric pattern of *L. emarginata*, while only five of these modulators have been shown to have an effect on similar preparations in *P. producta* (Dickinson et al., 2008; Miller, 2018). We expected all neuromodulators to modulate the pyloric pattern in *C. opilio*, as it is an opportunistic feeder like *L. emarginata*.

Multiple mechanisms could potentially explain interspecific differences in the extent to which the STNS is modulated. For example, there could be a lack of some modulators in the STNS of specialist feeders. Mass spectrometry data from the secretory tissues of *P. producta* reveal that this is not the case, as modulators are still expressed even if they have no effect on the pyloric pattern (Dickinson et al., 2008). Alternatively, different amounts of neuromodulator may be released by secretory tissues between species. Fixed amounts of modulators are applied during physiological recordings, which should control for differences in the amount of modulator release. We hypothesize that the lack of STNS sensitivity to a neuromodulator is due to a lack of neuromodulator receptors in the STG, although there may be receptors in other tissues. As a specialist feeder related to opportunistic feeders, it is plausible that *P. producta* evolved an herbivorous diet as a result of environmental pressures. As diet became restricted, the extensive modulation of digestive movements, by way of the pyloric pattern, became obsolete. Therefore, certain neuromodulator receptors in the STNS may not have been selected for.

Although receptors may be expressed in other nervous tissues, differential expression of receptors in the STG may explain the differing ranges of neuromodulator sensitivity between species. Assembly of a tissue-specific *de-novo* transcriptome allows for a rich analysis of modulator expression levels and their sequences, among crustacean species. This study uses unpublished data from previously assembled tissue-specific transcriptomes of *P. producta* and *L.*

emarginata to mine for modulator sequences (Miller, 2018). Additionally, *de-novo* transcriptomes were assembled for *C. opilio* brain and eyestalk tissues and mined for the same sequences. By first determining the sequences of modulators used in this study and potential physiologically-relevant peptides to use in future physiological studies, and then determining sequences of their respective receptors, a clear picture of the neuropeptidome of these Majoidea superfamily members can be elucidated. Using qPCR methods in the future, with the receptor sequences deduced through transcriptome mining as primers, on isolated stomatogastric ganglia, we will be able to examine the expression levels of each modulator receptor relative to housekeeping genes (Marder and Bucher, 2007). Receptors are expected to have little to no expression in the STG if their ligands have no measurable effect in isolated STNS preparations. As opportunistic feeders, *C. opilio* and *L. emarginata* should have similar expression of neuromodulator receptors in the STG. Specialist feeding crabs, such as *P. producta*, are predicted to have lower expression of receptors for neuromodulators that did not affect the pyloric pattern in STNS preparations.

METHODS

Animals

Adult male snow crabs (*C. opilio*), which were trapped in the Gulf of St. Lawrence, were purchased from a commercial seafood distributor (Fisherman's Market International, NS, Canada) in Halifax, Nova Scotia. Carapace widths of *C. opilio* specimens ranged from 12.4 - 15.2 cm. The crabs were housed in temperature-controlled seawater aquaria at a temperature of 4-10° C in Bowdoin College, Brunswick, ME. The crabs were fed defrosted scallops weekly and tank water was changed as needed, based on detritus buildup.

Portly spider crabs (*L. emarginata)* were obtained from Gulf Specimen Marine Lab, Inc. (Panacea, FL, USA) and housed in seawater aquaria at a temperature of 15-20°C, as these crabs live in warmer waters, in Bowdoin College, Brunswick, ME. Two males and one female crab were used in this study, with carapace widths ranging from 5.0 – 7.7 cm. Spider crabs were fed weekly with defrosted diver scallops and tank water was changed as needed.

Dissection

Each crab was removed directly from the tanks and anaesthetized on ice for 30-45 minutes. The foregut was removed from the animal with the mandibles intact to preserve the commissural ganglia. Lateral and medial cuts were made, and gastric mill teeth removed, in order to flatten the foregut. The foregut was then pinned interior side down in a Sylgard-lined Pyrex Dish and bathed with physiological saline (composition in mM: NaCl, 440.0; KCl, 11.0; $CaCl_2$, 13.0; $MgCl_2$, 26.0; Trizma base, 12.0; maleic acid, 1.22; pH: 7.4–7.5). This saline was originally optimized for physiological use in *Cancer borealis* crabs (Hooper and Marder, 1987). A fine dissection was then performed to isolate the stomatogastric nervous system from the foregut. Immediately after dissection, the nerve sheath around the STG was removed, in order to allow neuromodulators to reach somatic or dendritic receptors.

Electrophysiology

Using the same techniques optimized for neurophysiological studies in *P. producta* and *L. emarginata*, extracellular motor nerve activity was recorded from the lateral ventricular nerves (*lvn*) and medial ventricular nerves (*mvn*). When possible, activity was also recorded from the pyloric dilator nerve (*pdn*) or lateral pyloric nerve (*lpn*). Petroleum jelly wells were created around STNS motor nerves and bipolar stainless steel pin electrodes were placed in the wells to measure action potentials from each nerve. Electrical activity was amplified with a Model 1700 A-M Systems differential AC amplifier (Sequim, WA, USA), and recorded in Spike 2 (v9) through CED micro 1401 digitizer boards (Cambridge Electronic Design, Cambridge, UK). The preparations were superfused with chilled physiological saline at a rate of 6 mL/min throughout recording.

Neuromodulators

Seven neuromodulators were examined in this study. Five were neuropeptides, custom synthesized by Genscript (Piscataway, New Jersey, USA): *Cancer borealis* tachykinin-related peptide Ia (CabTRP Ia; APSGFLGMRamide), crustacean cardioactive peptide (CCAP; PFCNAFTGCamide), proctolin (RYLPT), myosuppressin (pQDLDHVFLRFamide), and red pigment concentrating hormone (RPCH; pELNFSPGWamide [in 0.01% dimethyl sulfoxide; Dickinson et al. 2008]). Neuropeptides were stored in 10^{-3} mol/L aliquots at -20°C and diluted to 10^{-6} mol/L just before application in physiological saline. Additionally, dopamine (Sigma-Aldrich; catalog no. H-8502, concentration of 10^{-4} mol/L) and the muscarinic acetylcholine receptor agonist oxotremorine (Sigma- Aldrich; catalog no. O-9126, concentrations of 10^{-6} and 10^{-7} mol/L) were tested. All neuromodulators were tested on *C. opilio* preparations. Only the neuropeptide myosuppressin was tested on most *P. producta* preparations as responses to the

other six neuromodulators have been previously reported (Dickinson et al., 2008). Each neuromodulator was superfused onto the preparation through a peristaltic pump for 10 minutes. Immediately after each application, the preparation was washed with normal saline for 50 minutes.

Intact vs. blocked conditions

After recordings were taken, the stomatogastric nerve was cut. This functionally removed anterior inputs from the commissural and esophageal ganglia. Since these ganglia provide the biggest source of modulatory inputs in the STNS, blocked preparations contain fewer sources of neuromodulatory input. Neuromodulators were reapplied to the preparation in order to study the effects of a single neuromodulator at a time.

Analysis of physiological recordings

After electrical activity was recorded, a variety of neuronal firing parameters were analyzed to determine whether each neuromodulator had an effect on the pyloric pattern in *C. opilio*. The same parameters used in the analysis of *L. emarginata* and *P. producta* were measured to allow for direct comparison (Miller, 2018). These parameters were quantified directly in Spike 2 for each motor neuron in the pyloric network and include burst duration, duty cycle, cycle period, and spike frequency. Cycle frequency of the pattern was quantified using the cycle period of PD, as this neuron is the pacemaker of the pyloric pattern. Quantification was performed using scripts that were created by the Bucher laboratory at Rutgers University and are available to the public (http://www.stg.rutgers.edu/Resources.html). In order to quantify differences in firing patterns before and after neuromodulator application, 10 cycles of the pyloric pattern were averaged immediately before, during, and around 40 minutes after neuromodulator application. Statistical analysis, including paired t-tests of each parameter

immediately before and during neuromodulator application, and graphing of results were performed in RStudio (RStudio Inc, Boston, MA, USA) using the R language (R Core Team, 2017).

C. opilio RNA isolation and next-generation sequencing

Total *C. opilio* RNA was isolated from brain and paired eyestalk tissue using either the Takara Nucleospin RNA isolation kit (Takara Bio Inc. Kusatsu, Japan) or the Qiagen RNeasy series RNA isolation kits (QIAGEN N.V, Hilden, DE, USA). Tissue samples were homogenized using 3.0 mm Triple-Pure (Molecular Biology Grade) Zirconium Bead tubes (#D1032-30, Benchmark Scientific Inc, Sayreville, NJ, USA) filled with either 300 µL of Takara RA1 Lysis Buffer (for Takara Nucleospin extraction) or 1 mL of QIAzol Lysis Reagent (for Qiagen RNeasy extraction). Samples were homogenized while in bead tubes using a Model D1030 2700 rpm BeadBug Microtube Bead Homogenizer (Benchmark Scientific Inc, Sayreville, NJ, USA) for three minutes total in 15 second intervals followed by 15 second intervals on ice. RNA extraction was performed following the manufacturer's specifications. Final elution was performed by running 30 µL of RNAse-free deionized H_2O through the column matrix twice. Sample concentration and quality were assessed with an Agilent 4200 Tapestation (Agilent Technologies, Santa Clara, CA, USA) with a standard sensitivity RNA ScreenTape Assay protocol. Samples were deemed high quality if three distinct peaks between 1,500 and 2,500 nucleotides were observed, and little signal was observed at other nucleotide lengths. Total RNA sample were stored at -80°C.

Total RNA samples were sent to Admera Health (South Plainfield, NJ, USA) for sequencing. Samples were purified using oligo-dT selection (polyA enrichment with oligodT beads) in order to isolate mRNA. Double-stranded cDNA libraries were then generated from

purified mRNA using the KAPA Stranded mRNA-seq kit (#KK8420, Kapa Biosystems Ltd, Wilmington, MA, USA). Finally, samples were sequenced using Illumina Inc. Next-Generation Sequencing (San Diego, CA, USA) with paired-end 150 bp reads on a single flow cell.

C. opilio tissue-specific transcriptome assembly

Raw reads from the RNA-seq analysis were first assessed for quality using the FASTQC program (v0.11.9) in order to identify faults in the sequencing. Illumina sequencing adapters were trimmed from all sample reads using the paired-end ILLUMINACLIP function in Trimmomatic with the TruSeq 3 preset (Bolger et al., 2014). No further quality culling was performed, as no mean Phred scores fell below 30 throughout the length of each read, forward or reverse. Adapter sequence trimming reduced the number of reads per sample from 45-64 million reads to 36-51 million reads. After trimming, reads were quality checked again using FASTQC. Additional adapter trimming was needed, and Trimmomatic was performed again using the custom adapter sequences provided by the sequencing site as queries. *De novo* transcriptome assembly was performed using Trinity software (v2.8.4) (Grabherr et al., 2011). The program was run on the Bowdoin College High Performance Computing (HPC) Linux Grid (Brunswick, ME, US). Each node in the grid consists of 16-56 CPU cores with 192-384 Gb of RAM, for a total of 1304 cores across all nodes. For assembly, tissue-specific sample reads were combined into a single forward read fastq file and a single reverse read fastq file. A separate transcriptome was created for brain and eyestalk tissue, using the parameters: max memory, 200 G; CPU 40. No read coverage or contig length requirements were set for assembly.

In order to reduce the high redundancy observed in the transcriptome of *C. opilio*, similar nucleotide sequences were clustered based on global sequence identity using the CD-HIT program (v4.8.1) (Fu et al., 2012). The CD-HIT-EST protocol was used with a sequence identity

threshold of 0.90, so as to reduce to the number of reported transcript isoforms, and a word length of 9. It was run on the Bowdoin College HPC Linux Grid with 16 GB of memory allocated to 8 CPUs.

Statistics on alignment and mapping were obtained in multiple ways. First, the Trinity Toolkit's built-in Perl script trinitystats.pl was used to understand the number of contigs, Trinity 'genes' and the distribution of contig lengths. Similar information on contig size was obtained through provided CD-HIT clustering statistics output. In order to determine read support and mapping information, we used Bowtie2 (v2.4.1) to index each transcriptome and align trimmed reads back onto the unclustered transcriptome, with the parameters: parallel_threads = 40, search for up to 20 alignments per read (-k mode = 20) (Langmead and Salzberg, 2012). The read alignment statistics were captured into a single text file through SAM Tools, with suppression of reads that fail to align (v1.4) (Li et al., 2009). Alignments were sorted by coordinate and indexed along with the transcriptome to visualize reads on Trinity contigs graphically using Integrative Genomics Viewer (IGV) (Thorvaldsdottir et al., 2013).

Two individual BUSCO analyses were performed on each *C. opilio* transcriptome, using BUSCO (v4.0.5) software installed in a miniconda3 virtual environment (Seppey et al., 2019). This quality metric assesses the presence of around 1,000 genes from a curated evolutionary dataset to provide an estimate of completeness for a transcriptome assembly. First, the complete transcriptomes prior to clustering were analyzed in transcriptome mode using the lineage dataset arthropoda_odb10 (2019-11-27). Second, candidate coding regions were predicted and translated into peptide sequences, from open reading frame length and base composition, using TransDecoder (v5.5.0) (reviewed in Haas et al., 2013). BUSCO analysis was performed again using the .pep multi-FASTA file output from TransDecoder as the input file in protein mode.

Note that BUSCO produces summary results which consist of the percent of BUSCO genes/proteins out of the total number of these (N) which are: complete (C), complete and single-copy (S), complete and duplicated (D), fragmented (F), or missing (M). Graphical representations of the distribution of BUSCO analysis results were generated using a provided Python script in the BUSCO package, generate_plot.py, which employs the R language and the data visualization package ggplot2 (R Core Team, 2017; Wickham, 2016).

Transcript abundances were calculated on a per sample basis for both transcriptomes using the Trinity Toolkit Perl script align_and_estimate_abundance.pl. This script was run using Kallisto (v0.46.0) on the Bowdoin College HPC Linux Grid, performing both reference preparation and alignment in a single run. Abundances per sample were concatenated and averages were calculated using the R language (R Core Team, 2017). Outliers were removed for each transcriptome by removing transcripts that were expressed on average less than 0.0000001 or greater than 1 time per million transcripts. Histograms were generated using the package ggplot2 in an R environment (Wickham, 2016).

Transcriptome mining for a prediction of the C. opilio neuropeptidome

BLAST databases were created for the eyestalk and brain transcriptomes after CD-HIT clustering. This was performed using the makeblastdb command in local command line BLAST+ software (v2.1.0) installed on the Bowdoin College HPC Linux Grid. Query neuropeptide sequences were obtained from either the published partial neuropeptidome for the eyestalk ganglia of the American lobster *Homarus americanus*, a closely related crustacean which likely has homologous peptide sequences, or from the published genome of *Drosophila melanogaster* through FlyBase.org (Christie et al., 2017; Thurmond et al., 2019). Using these query sequences, a tblastn protocol was performed in each transcriptome to determine major sequences.

Subsequent steps in establishing a neuropeptidome for *C. opilio* are identical to those taken in the mining of *L. emarginata* and *P. producta* transcriptomes as described below. Given the relatively short sequences of FMRFamide-like peptides, sequences containing the FLRFG sequence were searched for directly in the .pep multi-FASTA output of Transdecoder.

P. producta and L. emarginata transcriptome assembly (adapted from Miller, 2018)

Tissue-specific transcriptomes for both *P. producta* and *L. emarginata* were assembled as previously described in Miller, 2018. Briefly, total RNA was extracted from brain and STG tissues similar to as described above. Sequencing and library preparation was performed by the Georgia Genomics and Bioinformatics Core (University of Georgia, Athens, GA, USA). *De novo* assembly and initial transcriptome mining was performed as described in an earlier study (Christie et al., 2017).

Transcriptome mining for a prediction of the P. producta and L. emarginata neuropeptidome

Tissue-specific transcriptomes for brain and eyestalk tissue of *C. opilio*, brain and STG tissue of *P. producta,* and brain and STG tissue of *L. emarginata* were mined in order to determine the sequences of common signaling neuropeptides. Input prepro-peptide sequences were obtained from one of two sources: the published partial neuropeptidome for the eyestalk ganglia of the American lobster *Homarus americanus*, a closely related crustacean which likely has homologous peptide sequences, or from the published genome of *Drosophila melanogaster* through FlyBase.org (Christie et al., 2017; Thurmond et al., 2019). For *L. emarginata* and *P. producta,* input peptide sequences were BLASTed against the transcriptome of interest employing a tblastn protocol through BLAST software on an Intel-processor-based BEOWULF computer cluster (Pacific Biosciences Research Center, University of Hawaii at Manoa, Honolulu, HI, USA). The entire transcript from the result with the lowest Expect value was then

entered into the online sequence translation tool in ExPASy provided by the Swiss Institute of Bioinformatics (Artimo et al., 2012). The longest translated region in the correct reading frame, as given by tblastn output, was recorded as the pre-pro peptide sequence. Secretory signal peptide presence and sequence was confirmed using the SignalP service from the Center for Biological Sequence Analysis (v5.0 Technical University of Denmark, Lyngby, DK (Almagro Armenteros et al., 2019)). Using blastp in FlyBase, homologous *D. melanogaster* annotated proteins were established to provide ontology to the translated sequence. Homologous proteins were also searched for within published non-redundant arthropod genomes using the blastp protocol in BLAST from NCBI (U.S. National Library of Medicine, Bethesda, MD, US). Using the predicted neuropeptidome for *H. americanus*, the likely isoform sequence for which the peptide is named was identified and labeled (Christie et al., 2017). Mono- and di-basic cleavage sites were identified as one of: two sequential lysine residues; two sequential arginine residues; a lysine immediately followed by an arginine; or two lysine residues separated by 2, 4, or 6 amino acids (Veenstra, 2000). Any amino acids which were not considered to be part of the signal sequence, active peptide region, or cleavage sites are labelled as linker sequences.

RESULTS

Overview

Approximately 20% of the snow crabs obtained for this study died in tanks during the two months of data collection. There was no sign of zoological disease that could have affected other animals housed in the same tanks. Less than half of the data collected from snow crab preparations were analyzable. This was in part due to issues surrounding the use of a novel organism. Since *C. opilio* lives in ocean temperatures around 0°C, the preparations required strict temperature control which posed a challenge. Additionally, the foregut of *C. opilio* contained more layers of fat than has been observed in related crustacean species. The already torturous pathways of STNS motor nerves combined with the abundance of fatty tissue resulted in difficult dissections. In multiple preparations, the motor nerves and relevant ganglia were damaged during dissection, rendering those preparations unusable.

In the preparations that were analyzable, all seven neuromodulators elicited observable changes in the pyloric pattern. No single preparation was treated with all seven neuromodulators and the order of modulator application was randomized in each preparation. Not all neurons were recordable in all preparations, so n-values differ between preparations and modulators. The reported neuronal bursting parameters are consistent with those typically reported in STNS studies. Briefly, the duration of each burst, the spike frequency or the frequency of action potentials during each burst, and the duty cycle, or ratio of time in each burst where action potentials fire to the total burst duration, were calculated for each neuron type. These data are described below, separated by neuromodulator. For the core pyloric neurons (the LP neuron, PY neurons, and PD neurons), graphs of burst duration for each neuron type are shown. The average duration for one full pyloric cycle in seconds is also given as cycle period. Note that no burst

statistics calculated from *C. opilio* neurons changed significantly, according to a Wilcoxon signed rank-test, after modulator application.

Cancer borealis Tachykinin-Related Peptide Ia (CabTRP Ia)–C. opilio

In *stn*-intact preparations, CabTRP Ia excited the core pyloric pattern of *C. opilio* to a point that made individual spikes difficult to discern, rendering most preparations unanalyzable (Fig. 3). The core pyloric pattern could only be analyzed in a single preparation. In that preparation, PD spike frequency per burst increased by 30.0%, while LP spike frequency increased by 65.4% and PY spike frequency increased by 67.2%. The cycle frequency of the pattern decreased by 72.6% in the presence of CabTRP. VD burst parameters were only analyzable in a single preparation, different from the one described above. The duty cycle of the VD neuron increased by 26.6% in the presence of CabTRP Ia. The number of spikes increased from an average of 2.5 spikes per burst at baseline to an average of 5.8 spikes per burst and an increase in spike frequency per burst of 259.2%. The burst duration did not change in the presence of CabTRP Ia.

In three preparations, the *stn* was cut to remove anterior modulatory inputs, which eliminated patterned activity that was previously observed in the *lvn* and *mvn.* However, spontaneous tonic firing could be observed on the *lvn.* In the *stn*-blocked condition, CabTRP Ia did not activate the full pyloric pattern in any of these preparations on which it was tested. Spontaneous activity in the *lvn* increased in all three preparations after CabTRP Ia was administered, but the *mvn* remained silent (Fig. 4).

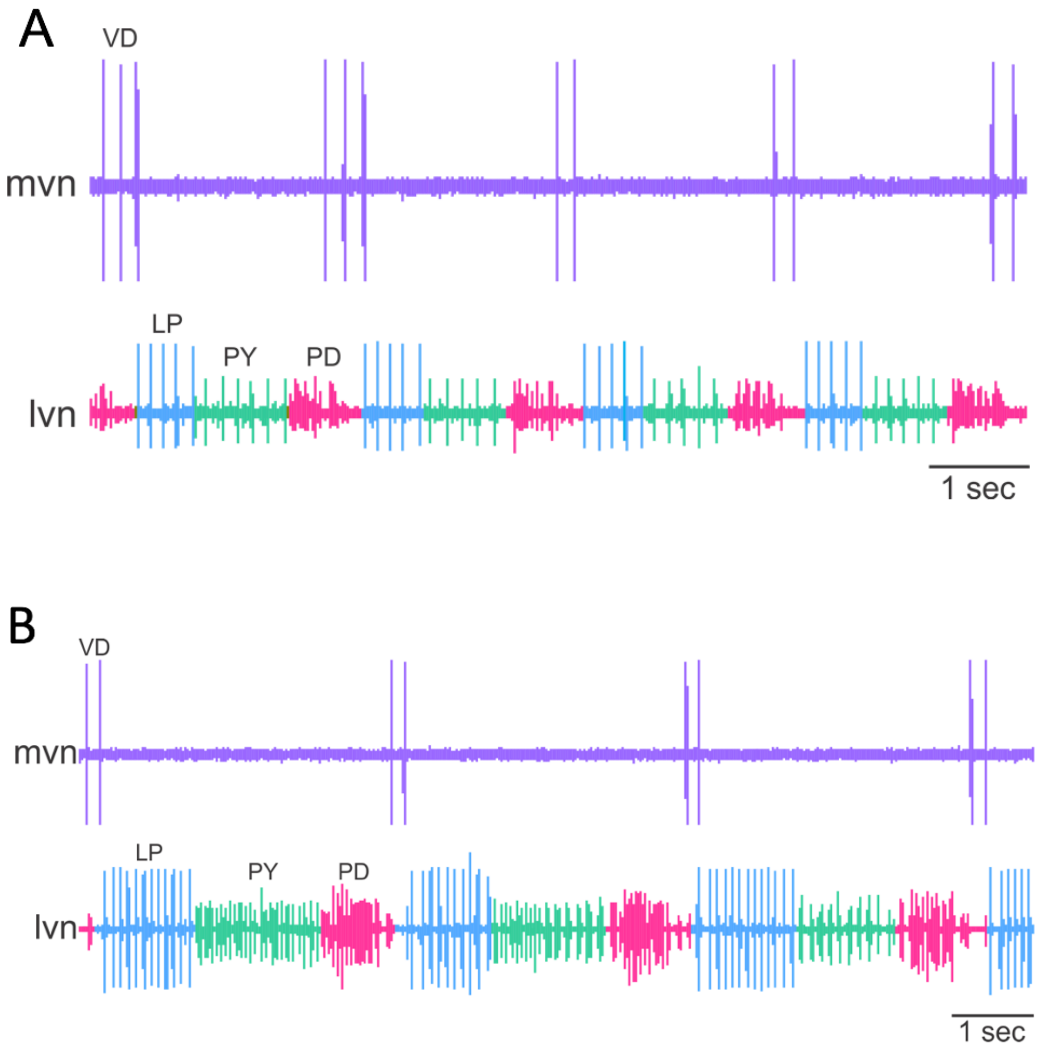

Figure 3. Extracellular recordings from the *mvn* and *lvn* in *stn*-intact *C. opilio* preparations before and after application of CabTRP Ia (10^{-6} M). **A)** Baseline recordings before the peptide application. **B)** Recording from nerves in the presence of CabTRP Ia.

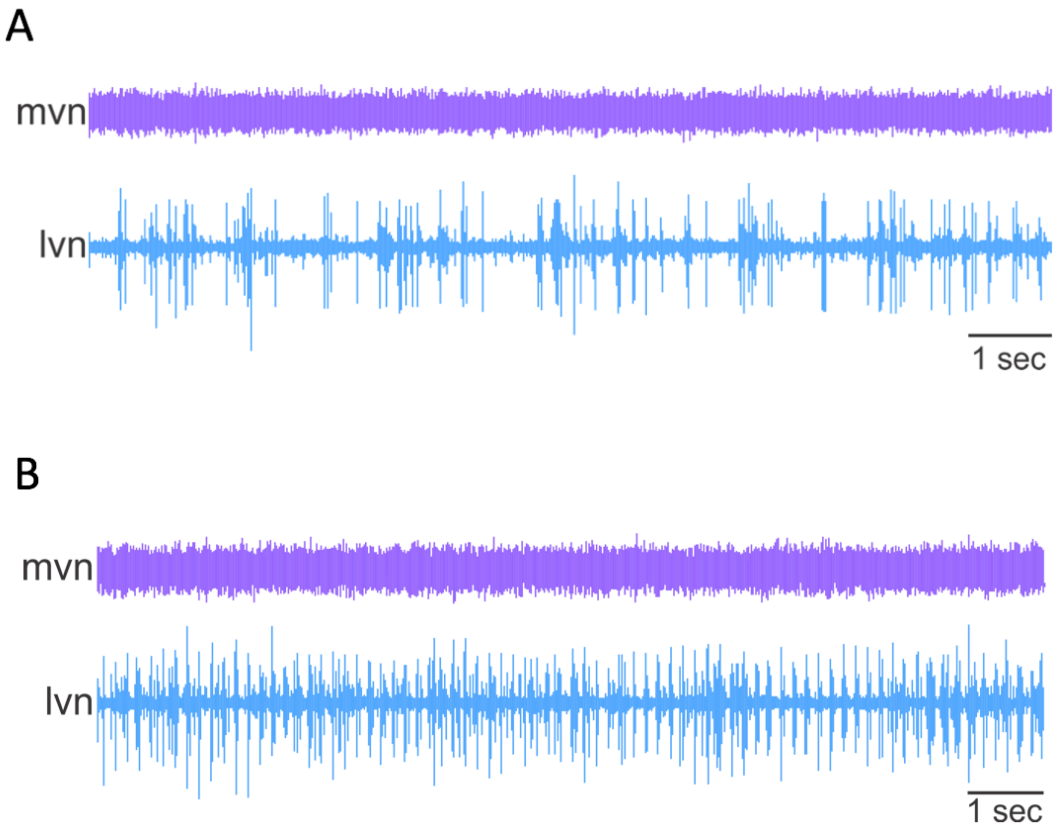

Figure 4. Extracellular recordings from the *mvn* and *lvn* in *stn*-blocked *C. opilio* preparations before and during application of the neuropeptide CabTRP Ia. **A)** Baseline recordings show no activity on the *mvn* and spontaneous, unpatterned firing on the *lvn.* **B)** In the presence of CabTRP Ia, no activity was observed on the *mvn,* but an increase of activity was observed on the *lvn*. The pyloric pattern was not activated.

Red Pigment Concentrating Hormone (RPCH)–C. opilio

In *stn*-intact preparations, RPCH appeared to modulate the pyloric pattern in *stn*-intact (Fig. 5). The burst duration of the LP neuron increased in two preparations, but decreased in one preparation during RPCH application (Fig. 6A). The LP neuron's spike frequency increased in three preparations in the presence of RPCH (Fig. 6B). There were no significant increases in any of the PY neurons' burst parameters, and burst duration could only be calculated in a single preparation. The PD neurons' burst duration increased in a single preparation and decreased in another (Fig. 6C). The pyloric pattern cycle period increased modestly in two preparations (n=2).

VD neuron firing was only observed in a single preparation, in which both its burst duration and duty cycle increased from baseline in the presence of RPCH (+254% and +230%, respectively, n=1), but the spike frequency per burst of the VD neuron decreased (-16.8%, n=1) in the single preparation in which it was recorded.

In the *stn*-blocked condition, RPCH activated the full pyloric pattern in one of three preparations (Fig. 7). In the other two preparations, there appeared to be an increase in spontaneous bursting as well as activation of gastric mill patterns.

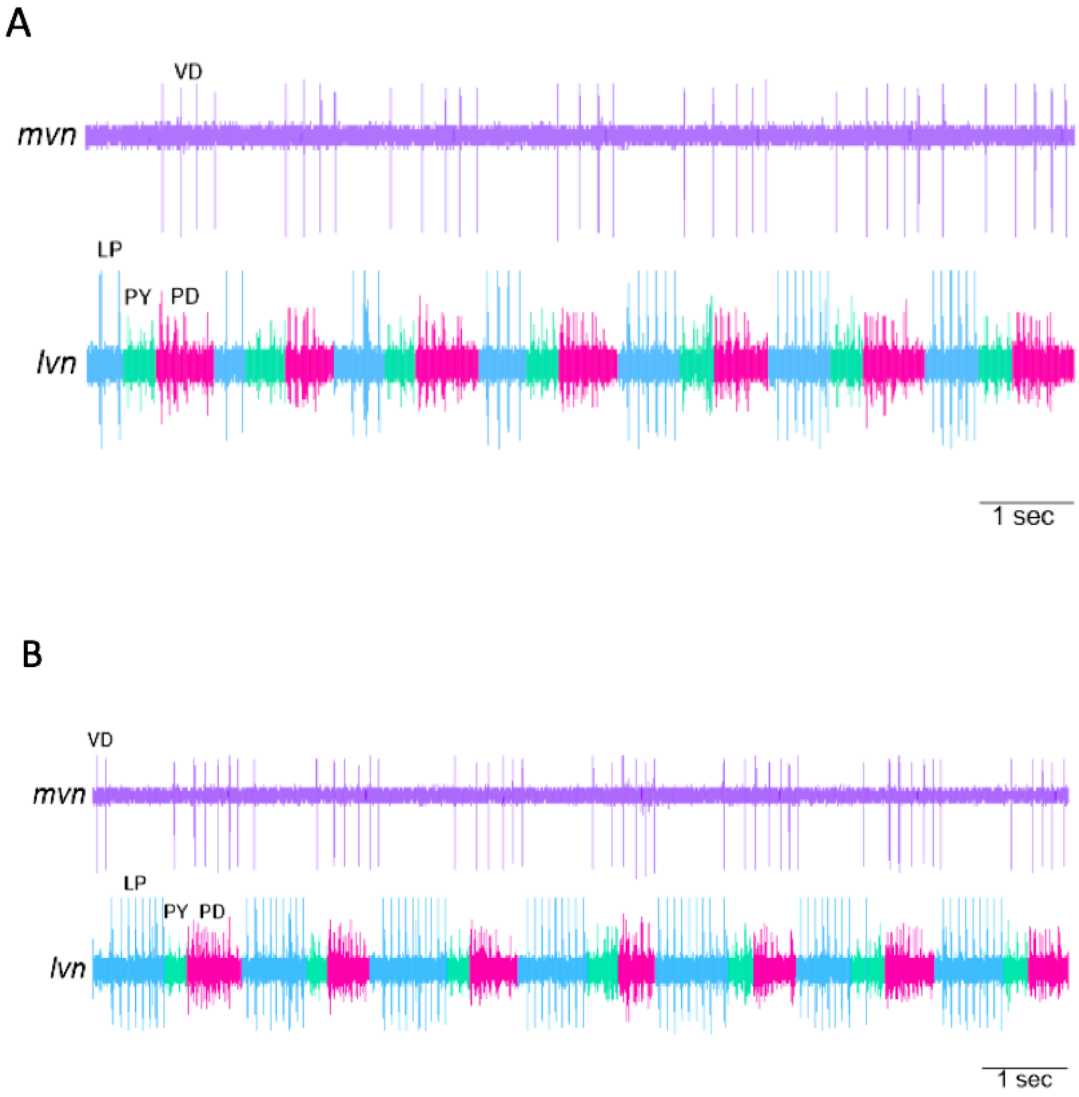

Figure 5. Extracellular recordings from the *mvn* and *lvn* in *stn*-intact *C. opilio* preparations before **(A)** and during application of RPCH (10^{-6} M) **(B)**. The number of spikes per burst as well as the burst duration of VD and LP neurons appears to increase in the presence of RPCH.

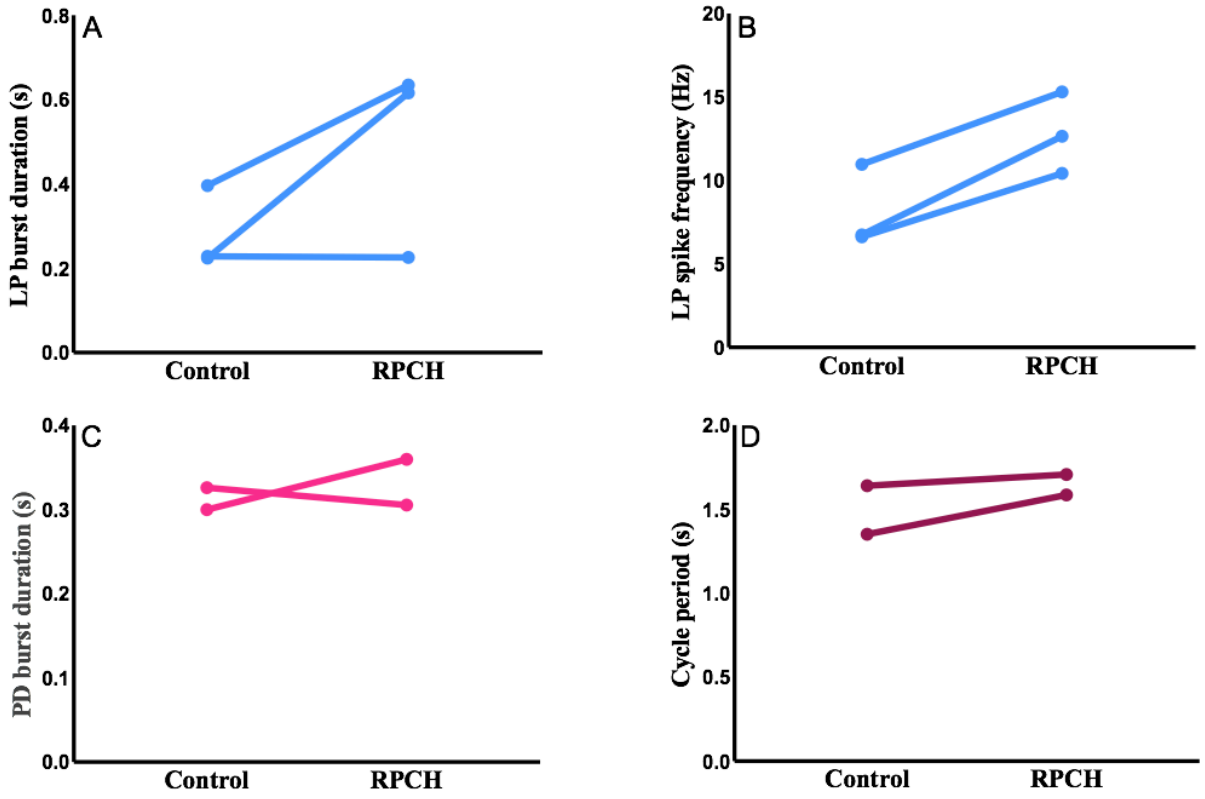

Figure 6. RPCH (10^{-6} M) appeared to modulate LP and PD neuron firing in *Chionoecetes opilio*. **A)** LP neuron burst duration increased in two preparations, but decreased in one presentation in the presence of RPCH (n=3). **B)** The LP neuron's spike frequency per burst increased in the presence of RPCH (n=3) C) PD neurons' burst duration increased in one preparation and decreased in another in the presence of RPCH (n=2). **D)** The cycle period of the pyloric pattern increased modestly in two preparations (n=2). None of these burst parameters are significantly different from baseline (Wilcoxon signed rank-test).

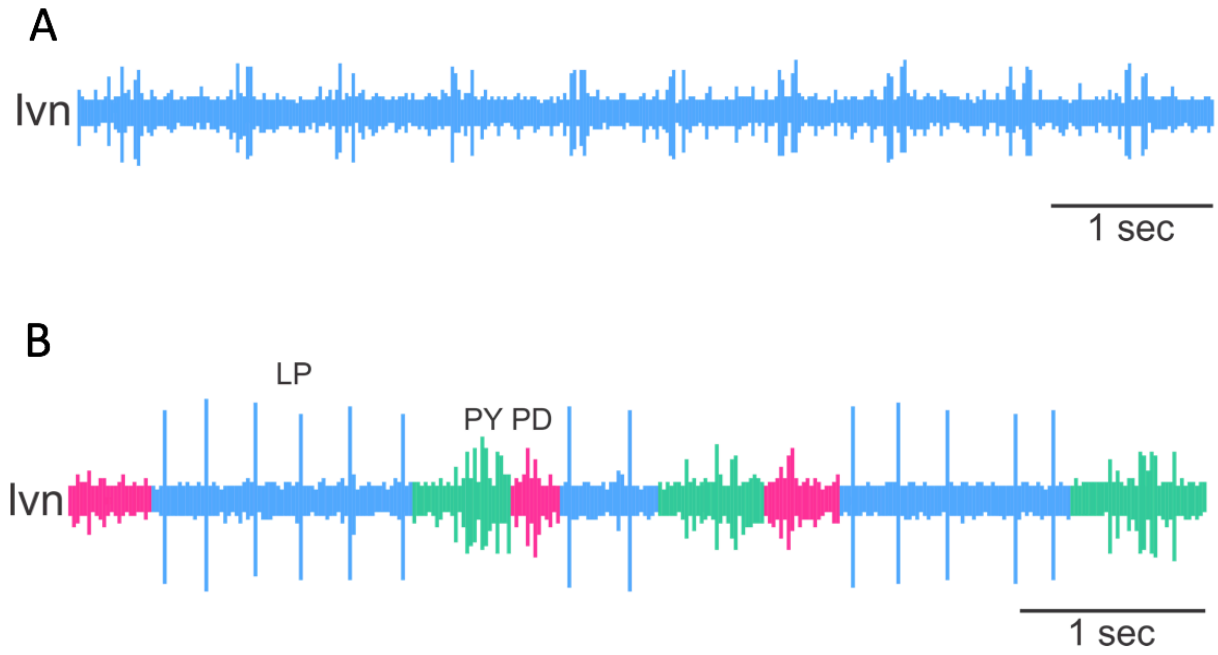

Figure 7. RPCH activates the pyloric pattern in *stn*-blocked *C. opilio* preparations. **A)** Baseline extracellular recordings taken before RPCH application. Patterned activity was observed, although the full pyloric pattern was not active. **B)** In the presence of RPCH, the pyloric pattern was activated, with firing from PD, LP, and PY neurons.

Proctolin–C. opilio

Proctolin appeared to modulate the pyloric pattern in *C. opilio* (Fig. 8). Proctolin increased the LP neuron's burst duration (Fig. 9A, n=2) and spike frequency (Fig. 9B, n=2) in *stn*-intact preparations. PY neurons' burst duration decreased in one preparation and increased in another (Fig. 9C, n=2). The burst duration of PD neurons increased slightly in the presence of proctolin (Fig. 9D, n=2). The pattern's cycle frequency remained unchanged after proctolin application (n=2). In one preparation, the pyloric pattern's cycle period decreased, while it increased in another (Fig. 9E). In the single preparation in which VD neuron firing was observed at baseline, VD neuron burst duration, duty cycle, and spike frequency all increased drastically after the introduction of proctolin (n=1, +251.8%, +337.1%, +76.7%, respectively). Proctolin did not activate the pyloric pattern in any of three blocked preparations; however, a marked increase in spontaneous activity was observed (Fig. 10).

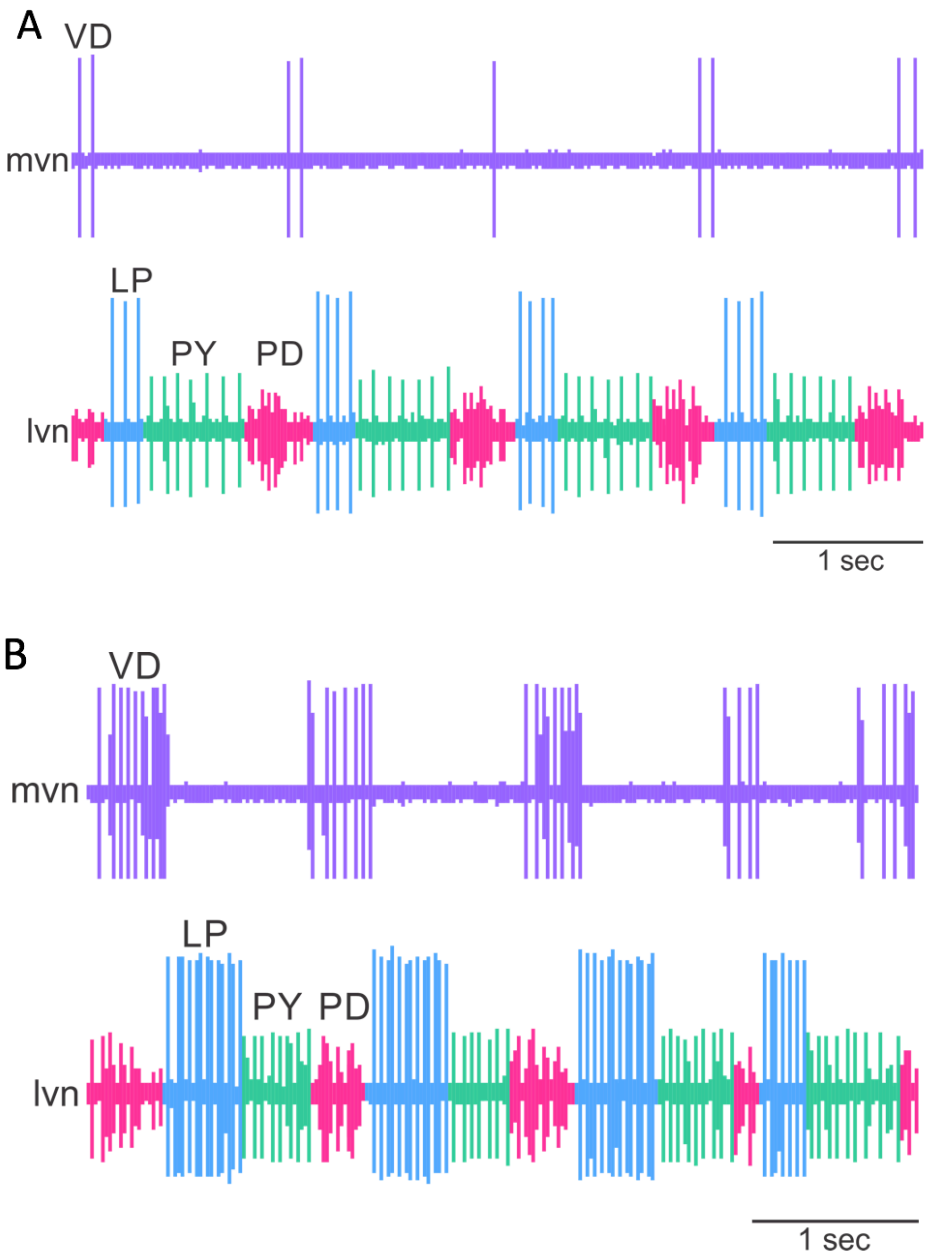

Figure 8. Extracellular recordings from the *mvn* and *lvn* in *stn*-intact *Chionoecetes opilio* preparations before and during application of the neuropeptide proctolin (10^{-6} M). **A)** Baseline extracellular recording before peptide application. **B)** In the presence of proctolin, burst duration of VD and LP neurons appear to increase while the burst duration of PY neurons seems to decrease.

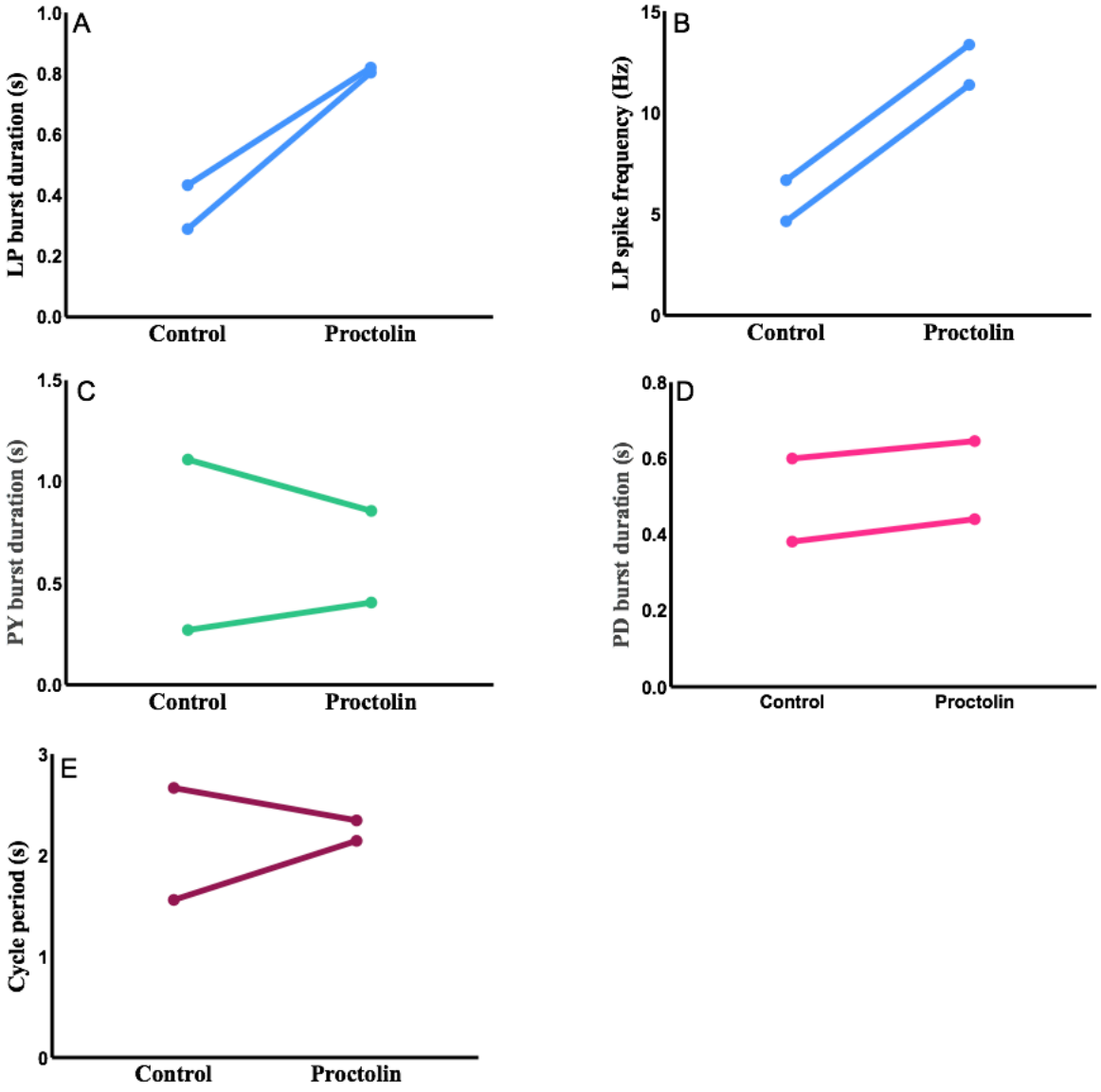

Figure 9. Proctolin (10^{-6} M) appeared to modulate the pyloric pattern in *Chionoecetes opilio.* **A)** The LP neuron's burst duration increased in two preparations in the presence of proctolin (n=2) **B)** The LP neuron's spike frequency increased in both preparations in which it was applied in the presence of proctolin (n=2). **C)** PY neurons' burst duration increased in one preparation and decreased in another the presence of proctolin (n=2). **D)** The burst duration of PD neurons increased slightly in the presence of proctolin (n=2). **E)** The cycle period of the full pyloric pattern increased in one preparation and decreased in another (n=2).

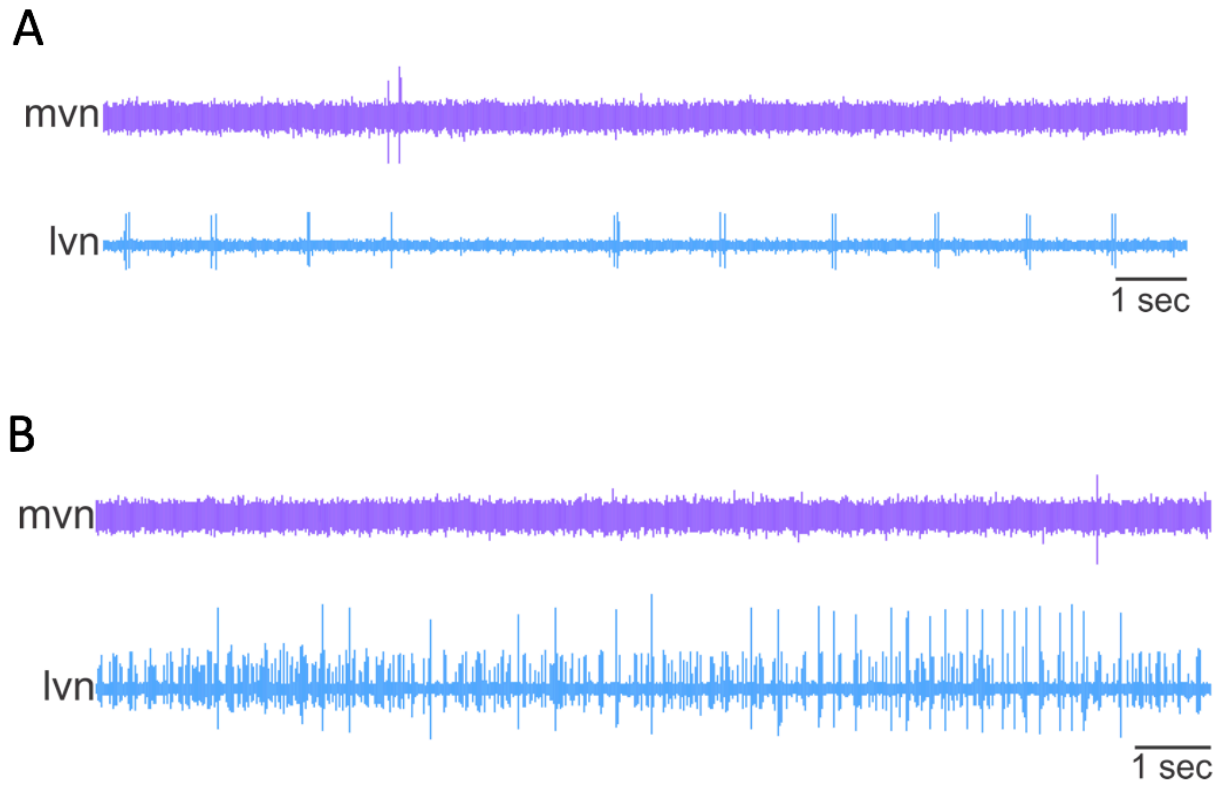

Figure 10. Proctolin 10^{-6} M did not activate the pyloric pattern in *stn*-blocked preparations of *C. opilio*. **A)** Baseline extracellular recordings before peptide application. **B)** Although the pattern is not activated, the *lvn* shows an increase in spontaneous activity from multiple neuron types in the presence of proctolin.

Crustacean Cardioactive Peptide (CCAP)–C. opilio

In *stn*-intact preparations, CCAP appeared to modulate the pyloric pattern (Fig. 11). There was no significant change in the LP neuron's burst duration; however, it decreased by a mean of 42.0% in two preparations and increased by a mean of 11.4% in two other preparations (Fig. 12A, n=4). The burst duration of PY neurons increased in the presence of CCAP (Fig. 12B, n=2). Similarly, CCAP elicited increases in the burst durations of PD neurons (Fig. 12C, n=2). In the presence of CCAP, the cycle period of the pyloric pattern increased (Fig. 12D, n=2). Firing in the VD neuron was only observed in a single preparation in which burst duration, duty cycle, and

spike frequency all decreased during proctolin application (n=1, -62.7%, -77.7%, -23.8%, respectively).

Additionally, CCAP appeared to modulate *stn*-blocked *C. opilio* preparations (Fig. 13). Although the pyloric pattern was not activated in any preparation, there was an increase in spontaneous activity in all preparations.

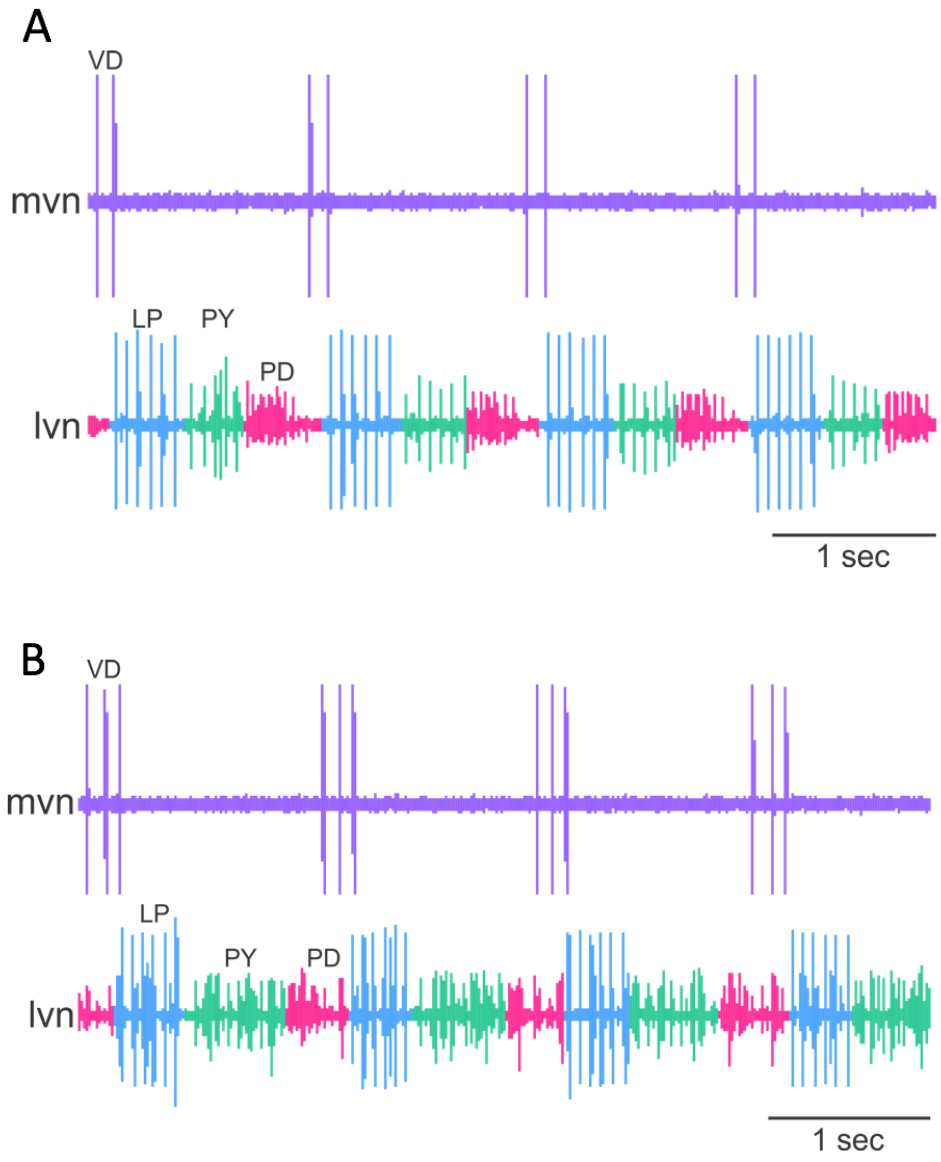

Figure 11. Extracellular recordings from the *mvn* and *lvn* in *stn*-intact *C. opilio* preparations before and during CCAP (10^{-6} M) application. **A)** Baseline recordings before the neuropeptide application. **B)** Recordings taken in the presence of CCAP. PY and VD burst duration seem to increase.

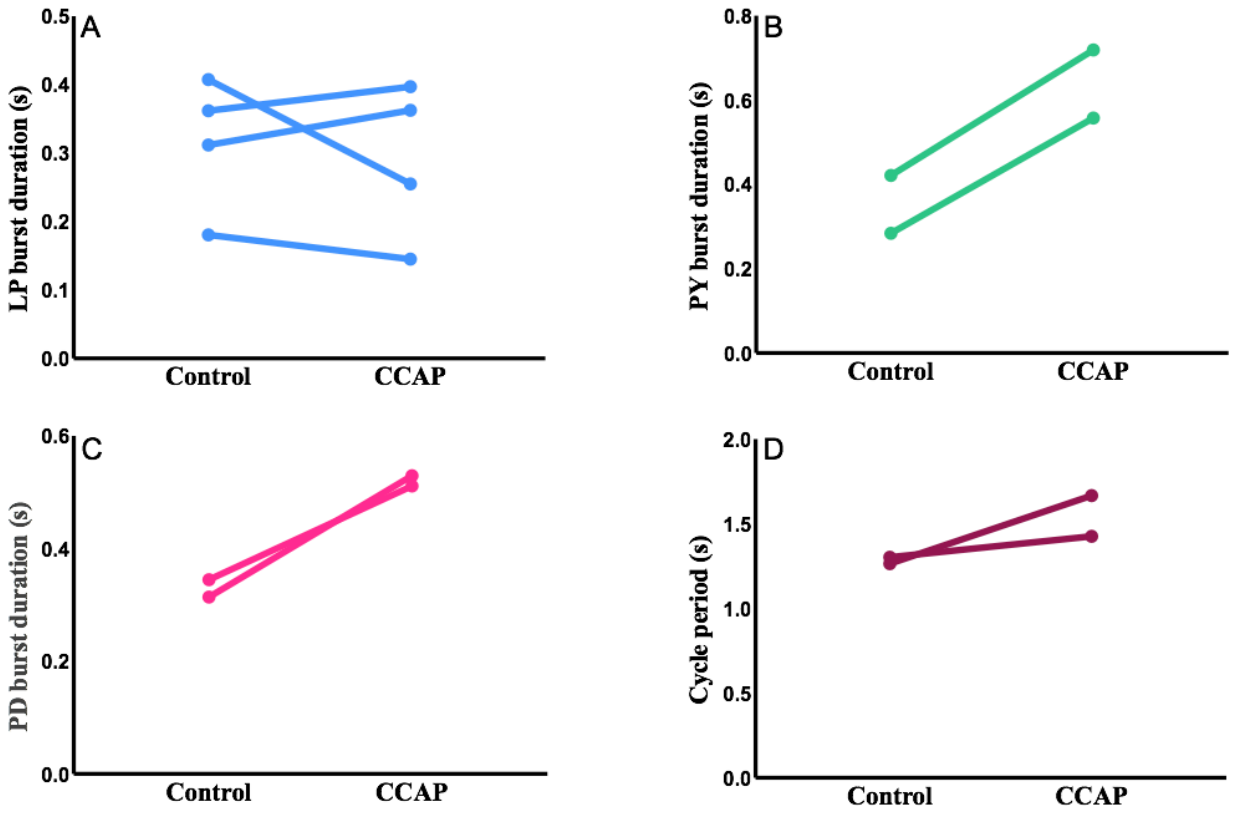

Figure 12. CCAP appeared to modulate the pyloric pattern in *Chionoecetes opilio*. **A)** The burst duration of the LP neuron increased in two preparations and decreased in two preparations in the presence of CCAP (n=4). **B)** PY neurons' burst durations increased in the presence of CCAP (n=2). **C)** The burst duration of PD neurons increased in the presence of CCAP (n=2). **D)** The cycle period of the pyloric pattern increased during proctolin application (n=2).

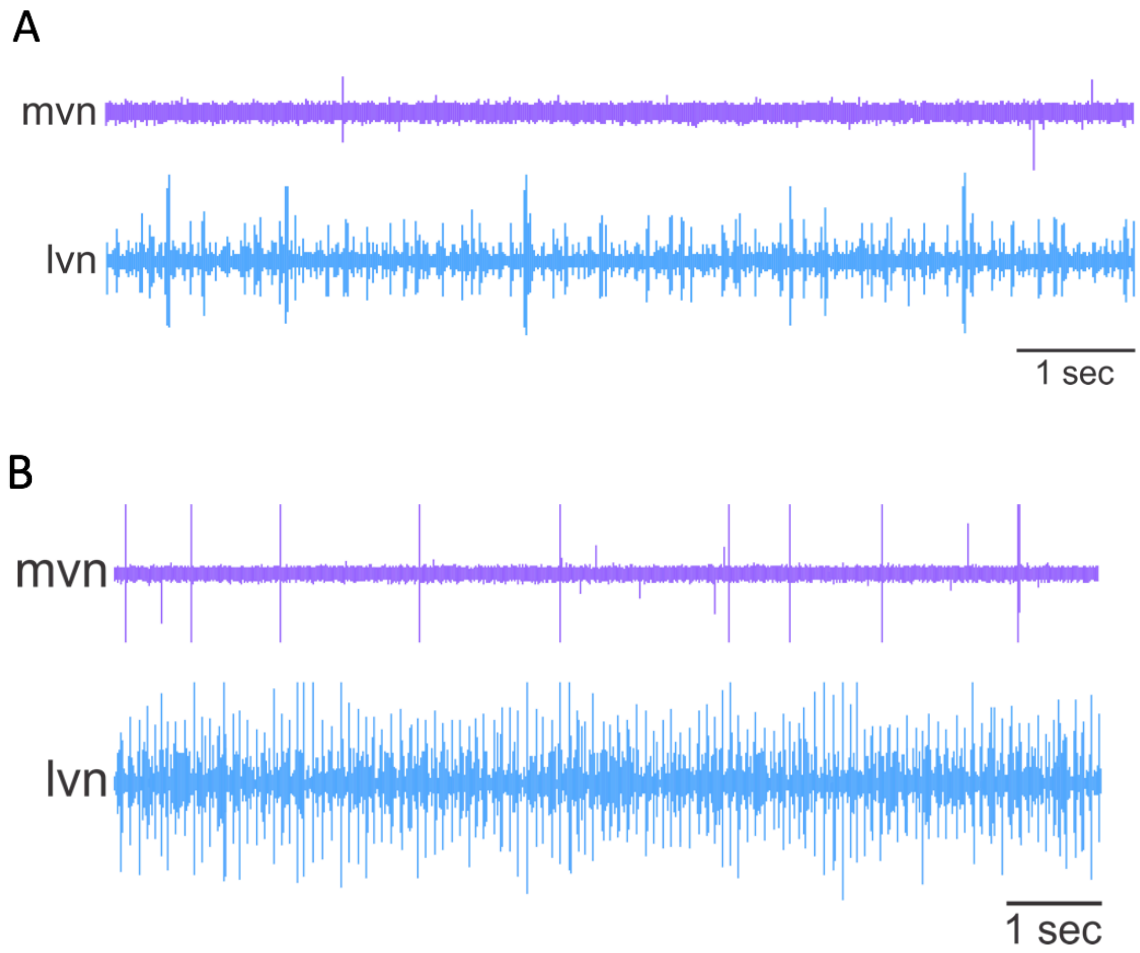

Figure 13. Extracellular recordings from the *lvn* and *mvn* in *stn*-blocked *C. opilio* preparations before and during CCAP (10^{-6} M) application. **A)** Baseline recordings before peptide application. Unpatterned spontaneous activity can be seen on the *lvn* with occasional VD or IC firing on the *mvn*. **B)** In the presence of CCAP, the pyloric pattern was not activated. However, spontaneous activity increases on both the *mvn* and *lvn*.

Dopamine–C. opilio

Dopamine was applied to three different, *stn*-intact snow crab preparations. In two preparations, dopamine modulated the pyloric pattern, but the preparation became unpatterned with rapid, spontaneous activity. In another preparation, the pyloric pattern cycle frequency increased by 288% when dopamine was applied. LP burst duration decreased (-44.1%), while duty cycle and spike frequency per burst increased in the presence of dopamine (+20.1% and +6.1%, respectively) (Fig. 14). In the same preparation, there was a decrease in PY burst

duration (-43.0%) and spike frequency (-25.4%), with an increase in PY duty cycle (+20.1%). PD burst duration increased in the presence of dopamine (+81.0%), while duty cycle (-10.9%) and spike frequency:(-28.6%) both decreased. VD burst statistics all increased in the presence of dopamine (burst duration: +321.8%, duty cycle: +351.8%, spike frequency: +8.3%). IC firing was not observed at baseline, but began to fire patterned bursts in the presence of dopamine between every two VD bursts. This IC firing subsided during the saline wash.

Dopamine was only tested in a single blocked preparation (Fig. 15). Although the pyloric pattern was not clearly observed, there was an increase in spontaneous activity.

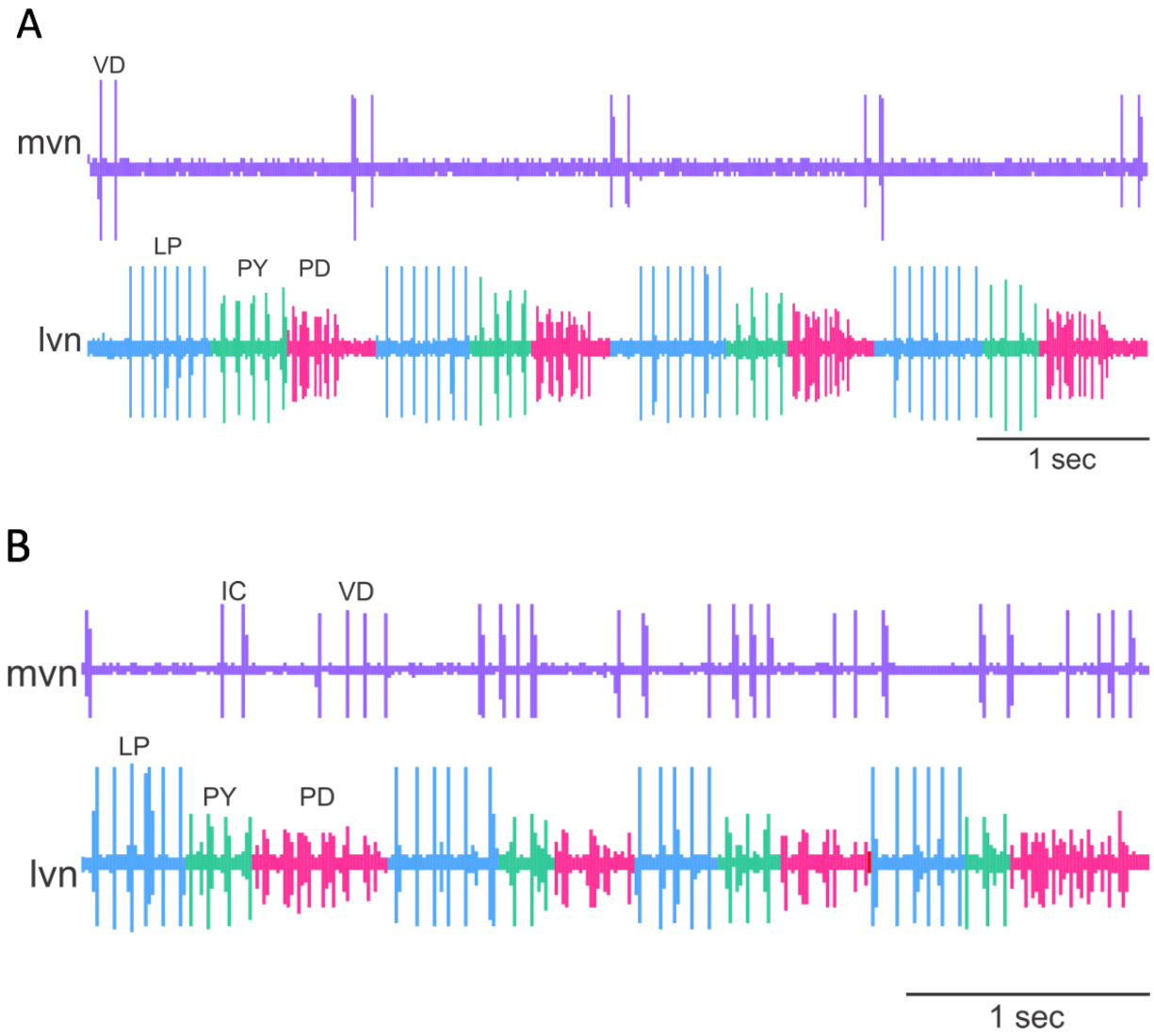

Figure 14. Extracellular recordings from the *mvn* and *lvn* in *stn*-intact *C. opilio* preparations before and during dopamine (10^{-4} M) application. **A)** Baseline recordings before amine application. **B)** In the presence of dopamine, LP spike frequency appears to decrease, while VD burst duration increases. Note that IC firing, which was not observed at baseline, is present in the presence of dopamine.

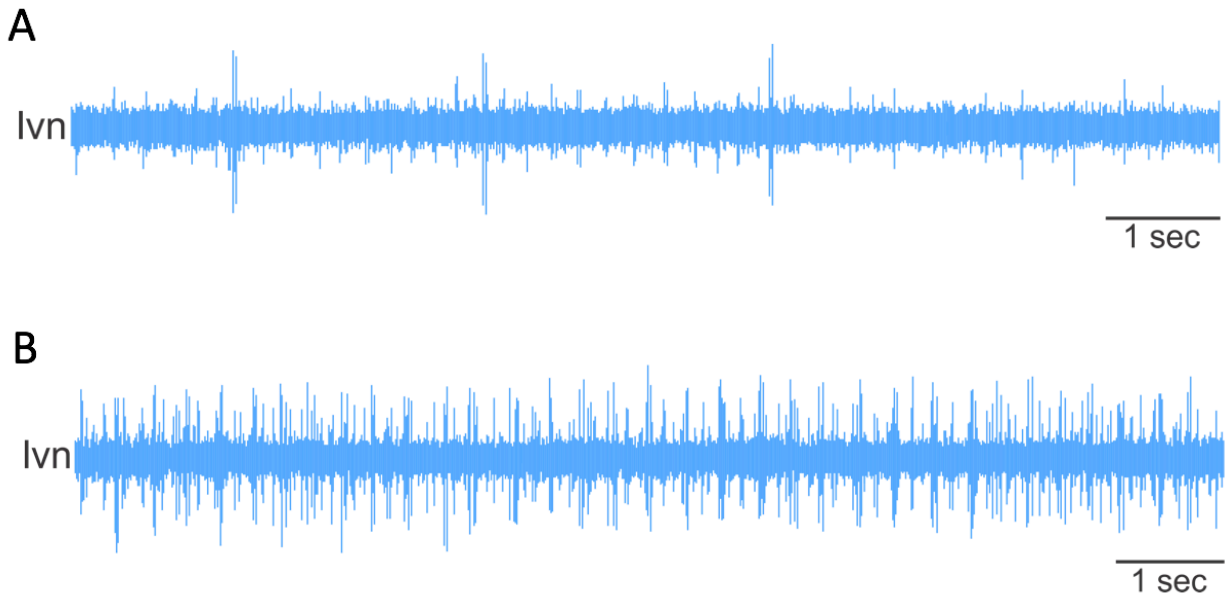

Figure 15. Dopamine (10^{-4} M) did not activate the pyloric pattern in *stn*-blocked *C. opilio* preparations. **A)** Baseline extracellular trace recording before modulator application. **B)** In the presence of dopamine, spontaneous activity on the *lvn* increases. The pyloric pattern was not activated.

Oxotremorine–C. opilio

The effects of the muscarinic acetylcholine agonist oxotremorine were so intense in some preparations that the pyloric pattern intermittently disappeared after periods of rapid activity. At a concentration of 10^{-6} M, oxotremorine was applied to two *stn*-intact preparations, neither of which were analyzable. In one of two preparations treated with 10^{-7} M concentrations of oxotremorine, only PD was analyzable (Fig. 16). In this preparation, PD spike frequency notably increased +128.1%. There were very slight and likely negligible changes in the other PD burst statistics. The cycle frequency of the pattern was relatively unchanged.

In *stn*-blocked preparations, oxotremorine activated the pyloric pattern in three of four blocked preparations (Fig. 17). Two of these preparations were treated with 10^{-6} M oxotremorine, while the third was treated with 10^{-7} M oxotremorine. In the fourth preparation, spontaneous activity seemed to increase after the application of oxotremorine 10^{-6} M.

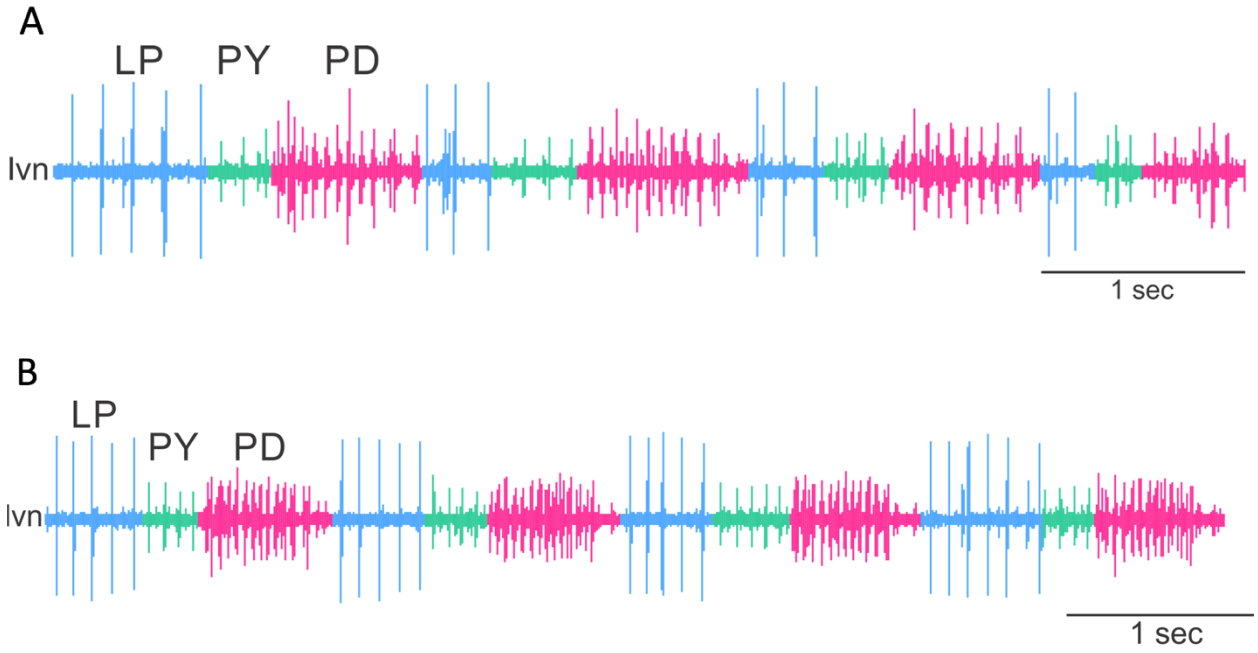

***Figure 16*.** Extracellular recordings from the *lvn* in *stn*-intact *C. opilio* preparations before and during application of the muscarinic acetylcholine receptor agonist oxotremorine (10^{-7} M). **A)** Baseline recording before application of oxotremorine. **B)** In the presence of oxotremorine, the number of spike per burst increases for all three core pyloric neurons. The burst duration of the PY and PD neurons appears to increase after modulator application.

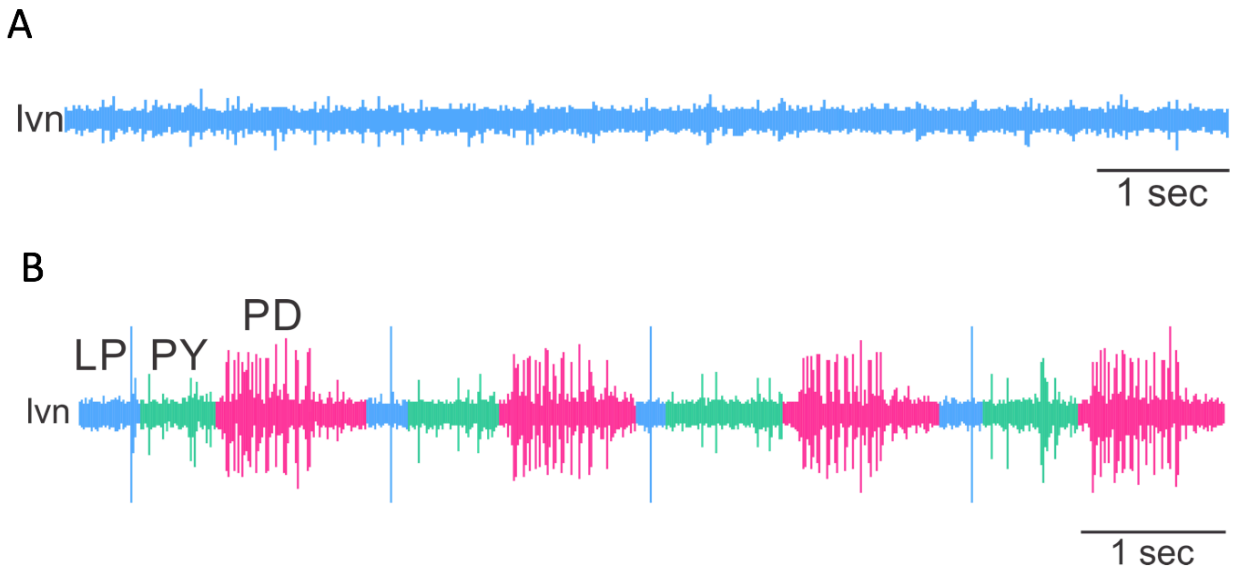

***Figure 17*.** Extracellular recordings from the *lvn* in *stn*-blocked *C. opilio* preparations before and during the application of the muscarinic acetylcholine receptor agonist oxotremorine (10^{-7} M). **A)** Baseline recording shows spontaneous activity on the *lvn*. **B)** In the presence of oxotremorine, the pyloric pattern was activated. Although bursting was not observed from the LP neuron, the triphasic core pattern is still discernable.

Myosuppressin–C. opilio

Of the four *stn*-intact *C. opilio* preparations in which myosuppressin (10^{-6} M) was tested, the pyloric pattern disappeared permanently in three preparations (Fig. 18). The pattern returned in one preparation, but the pattern was weak after lengthy saline washes and the preparation was discarded. Therefore, the burst statistics for myosuppressin's effects on the STG neurons could not be quantified. Due to the apparent inhibitory effects of myosuppressin, it was not applied to blocked preparations.

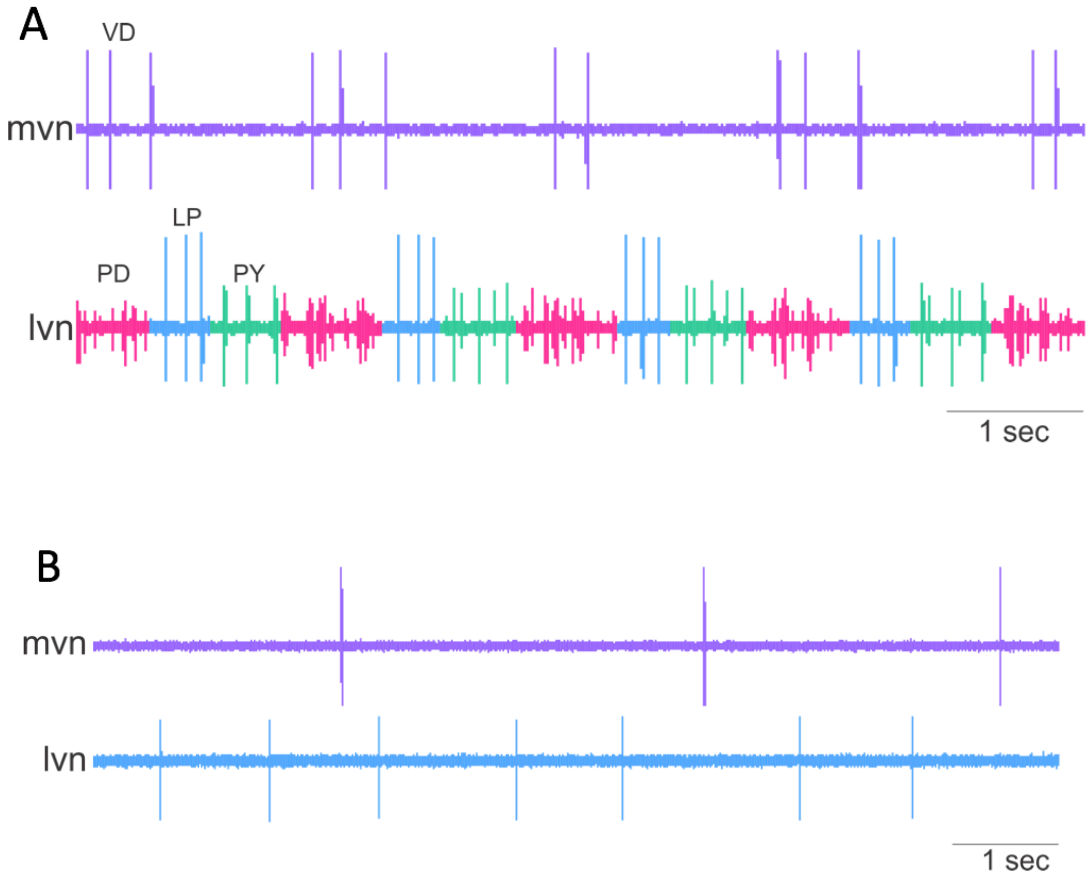

Figure 18. Extracellular recordings from the *mvn* and *lvn* in *stn*-intact *C. opilio* preparations before and during application of the neuropeptide myosuppressin (10^{-6} M). **A)** Baseline recordings before the application of myosuppressin. **B)** The pyloric pattern disappears in the presence of myosuppressin, leaving spontaneous, unpatterned firing in both the *mvn* and *lvn*. There is no bursting in either nerve.

In order to expand on previous work from the Dickinson lab examining this same suite of neuromodulators, this study also examined the isolated STNS of *Libinia emarginata* (Miller, 2018). Only two *stn*-intact preparations were recorded from in the presence of five neuromodulators, as unforeseen public health issues prevented continued data collection. These data were analyzed and combined with unpublished data from the Dickinson lab to provide a clearer picture of the modulatory capacity of *L. emarginata*. As was shown previously, all seven of these neuromodulators had a significant effect on the pyloric pattern. Combined results are shown below separated by neuromodulator; note that only those neuronal firing parameters that

were altered significantly by modulator application are shown. Results and analysis from the two neuromodulators not tested in the course of this study and sample extracellular traces from both *stn*-intact and *stn*-blocked conditions can be found in a previous undergraduate thesis from the Dickinson lab (Miller, 2018).

Cancer borealis Tachykinin-Related Peptide Ia (CabTRP Ia)–L. emarginata

CabTRP Ia was found to modulate the pyloric pattern of *stn*-intact *L. emarginata* in the total of 15 preparations that it was applied to. Of these preparations, LP firing was only observed in 14, and IC firing was only observed in 10. LP spike frequency increased in the presence of the modulator (Fig. 19A, n=14, paired t-test: p=0.0366). No other burst parameters were significantly altered in the LP neuron by CabTRP Ia. Similarly, only the spike frequency was affected by this modulator in IC neurons (Fig. 19B, n=10, pairedN t-test: p=0.0062). The only observed change in PY burst statistics was a decrease in duty cycle (Fig. 19C, n=15, paired t-test: p=0.0251). PD neuron firing decreased in duty cycle during bursts (Fig. 19D, n=15, paired t-test: p=0.0345), but no other changes in bursting characteristics were seen. VD firing was only observed in six preparations, and no significant changes occurred during CabTRP Ia application. The cycle period of the entire pyloric pattern was unchanged by the application of CabTRP Ia.

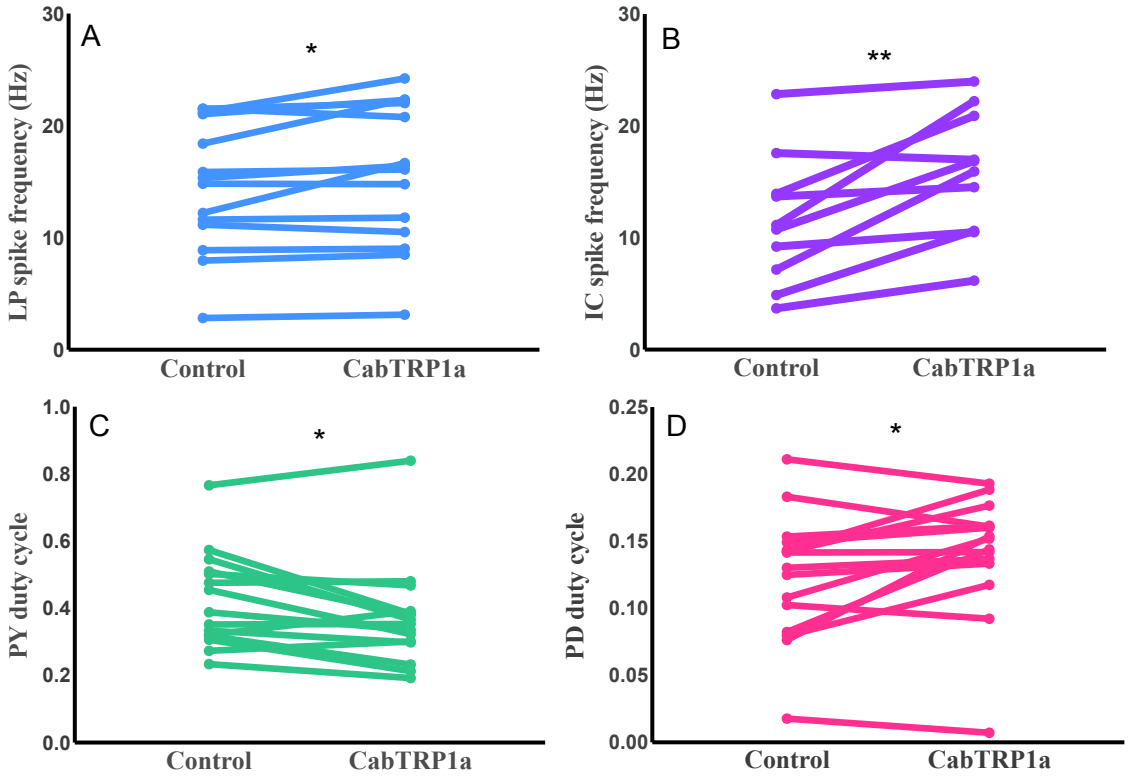

Figure 19. CabTRP Ia modulated the pyloric pattern in *Libinia emarginata*. **A)** LP spike frequency increased in the presence of CabTRPIa (n=14, paired t-test: p=0.0366). **B)** The spike frequency of IC neurons increased in the presence of CabTRP Ia (n=10, paired t-test: p=0.0062). **C)** The duty cycle of PY neurons decreased after CabTRP Ia application (n=15, paired t-test: p=0.0251). **D)** PD neurons' duty cycle decreased in the presence of CabTRP Ia (n=15, paired t-test: p=0.0345). * = $p \leq 0.05$; ** = $p \leq 0.01$

Red pigment concentrating hormone (RPCH)-L. emarginata

RPCH modulated the pyloric pattern of *L. emarginata* in 13 *stn*-intact preparations. In the presence of RPCH, the cycle period of the entire pyloric pattern decreased (Fig. 20A, n=10, paired t-test: p=0.0468). In LP neurons, both burst duration (Fig. 20B, n=13, paired t-test: p=0.0150) and duty cycle (Fig. 20C, n=13, paired t-test: $p \leq 0.0001$) increased, but spike frequency was unchanged. The spike frequency of PY neurons during bursts increased during RPCH application (Fig. 20D, n=9, paired t-test: p=0.0257), while no other PY firing characteristics were altered. IC neurons also exhibited an increase in spike frequency (Fig. 20E, n=10, paired t-test: p=0.0048) with no other significant changes to their firing parameters in the

presence of RPCH. VD neuron firing was only observed in four preparations; no significant changes were noted in the presence of RPCH.

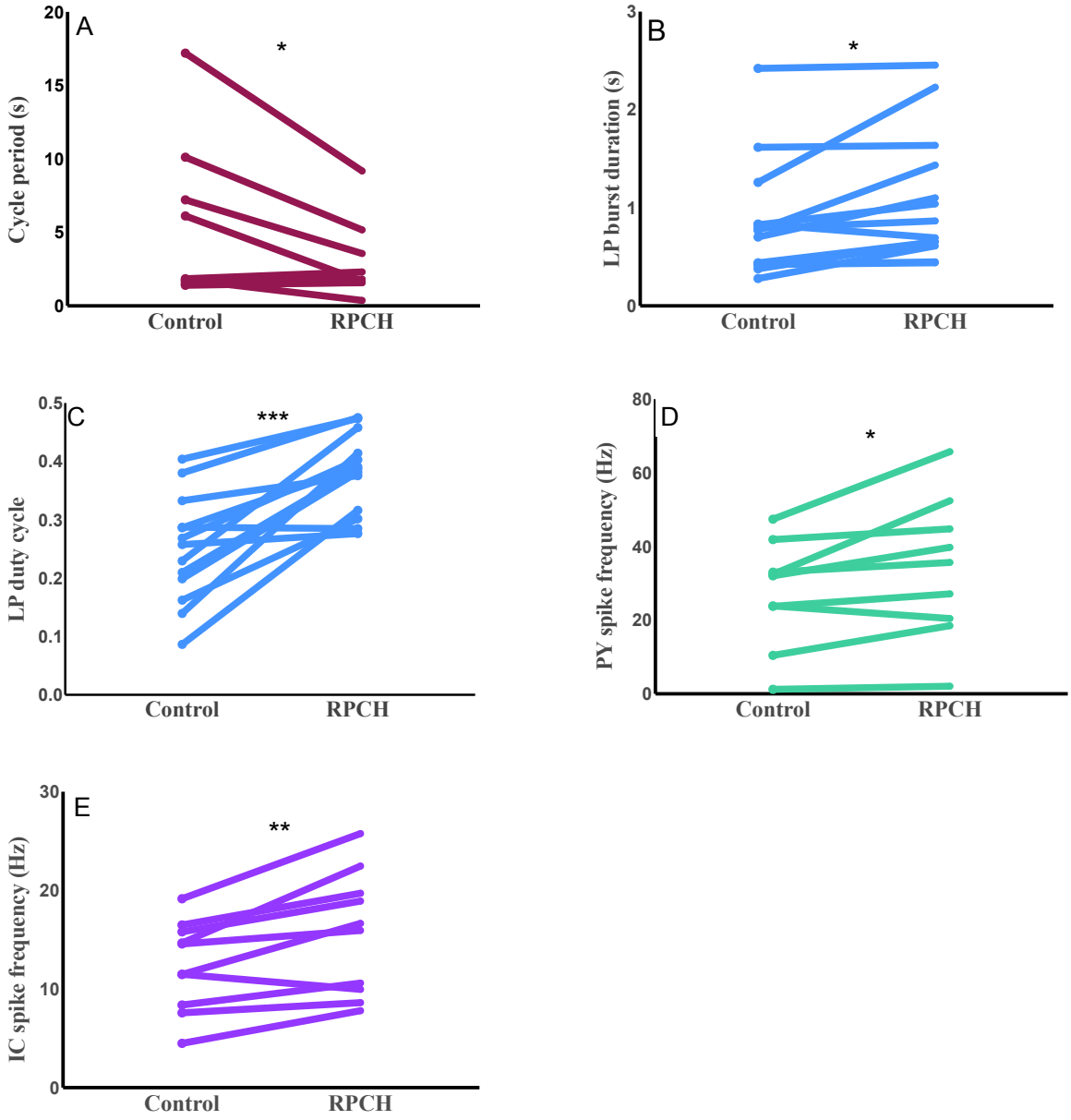

Figure 20. RPCH modulated the pyloric pattern in *stn*-intact *L. emarginata* preparations. **A)** The cycle period of the whole pyloric pattern decreased in the presence of RPCH (n=10, paired t-test: p=0.0468). **B)** Burst duration of LP neurons increased in the presence of RPCH (n=13, paired t-test: p=0.0150). **C)** The duty cycle of LP neurons increased in the presence of RPCH (n=13, paired t-test: p≤0.0001). **D)** In the presence of RPCH, the spike frequency of PY neurons increased (n=9, p=0.0257). **E)** The spike frequency of IC neurons increased in the presence of RPCH (n=10, p=0.0048). * = $p \leq 0.05$; ** = $p \leq 0.01$; *** = $p \leq 0.001$

Proctolin–L. emarginata

Proctolin was found to modulate the pyloric pattern in the 10 preparations of *L. emarginata* in which it was applied. There was no significant change in the cycle period of the entire pattern, as measured by PD neurons, before and after application of proctolin. In fact, no burst parameters of PD neurons were affected by proctolin application. In LP neurons, both the burst duration (Fig. 21A, n=9, paired t-test: p=0.0161) and duty cycle (Fig. 21B, n=9, paired t-test: p=0.0014) increased, but there was no effect of proctolin on spike frequency. During proctolin application, PY neurons exhibited a decrease in duty cycle (Fig. 21C, n=10, paired t-test: p=0.0132) and an increase in spike frequency (Fig. 21D, n=10, paired t-test: p=0.0136), but no change in burst duration. Similarly, IC neurons exhibited an increase in both duty cycle (Fig. 21E, n=8, paired t-test: p=0.0220) and spike frequency (Fig. 21F, n=8, paired t-test: p=0.0104) with no changes in burst duration in the presence of proctolin. Bursting in VD neurons was only seen in three of the 10 preparations, and no significant changes in bursting parameters were observed during proctolin application.

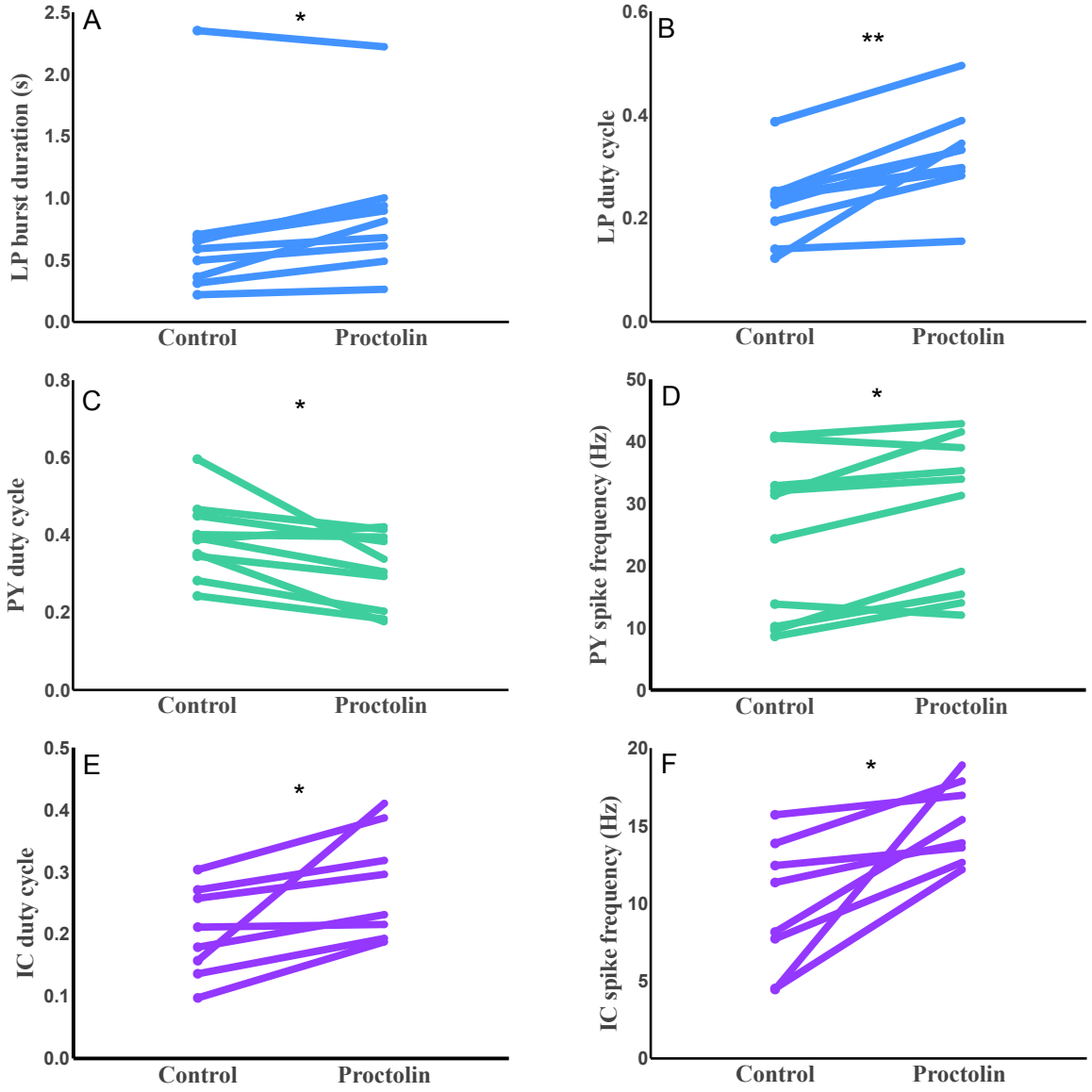

Figure 21. Proctolin modulated the pyloric pattern of *L. emarginata.* **A)** LP burst duration increased in the presence of proctolin (n=9, paired t-test: p=0.0161). **B)** LP duty cycle increased during proctolin application (n=9, paired t-test: p=0.0014). **C)** In the presence of proctolin, PY duty cycle decreased (n=10, paired t-test: p=0.0132). **D)** PY spike frequency increased in the presence of proctolin (n=10, paired t-test: p=0.0136). **E)** In the presence of proctolin, IC neuron duty cycle increased (n=8, paired t-test: p=0.0220). **F)** IC spike frequency increases in the presence of proctolin (n=8, paired t-test: p=0.0104). * = $p \leq 0.05$; ** = $p \leq 0.01$

Crustacean Cardioactive Peptide (CCAP)–L. emarginata

In all 15 *stn*-intact preparations, CCAP modulated the pyloric circuit of *L. emarginata.*

The cycle period of the pattern was not significantly changed by CCAP application. Firing on the

mvn was inconsistent in these preparations, as bursting in the IC neurons was seen in only 10 preparations and VD bursting was observed in only four preparations. LP neurons exhibited a decrease in burst duration (Fig. 22A, n=15, paired t-test: p=0.0496), but no other burst parameters were altered in the presence of CCAP. In the presence of CCAP, PD neuron spike frequency decreased (Fig. 22B, n=15, paired t-test: p=0.0007). No other significant changes were seen in PD neurons during CCAP application. During CCAP application, IC neurons showed a decrease in both burst duration (Fig. 22C, n=10, paired t-test: p=0.0022) and duty cycle (Fig. 22D, n=10, paired t-test: p=0.0291), but an increase in spike frequency (Fig. 22E, n=10, paired t-test: p=0.0081). VD neurons exhibited an increase in spike frequency (Fig. 22F, n=4, paired t-test: p=0.0024) in the presence of CCAP with no other burst parameters affected.

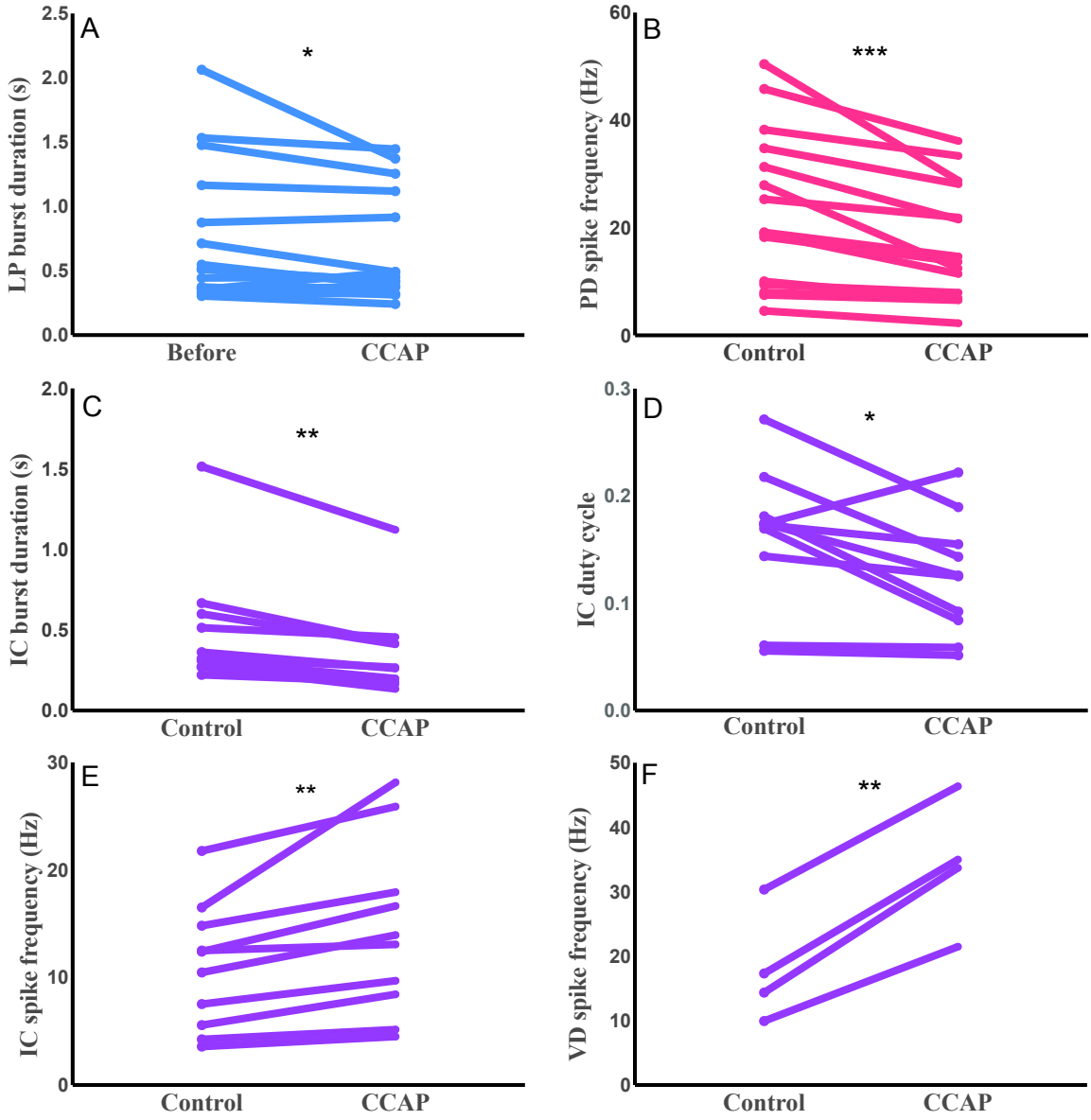

Figure 22. CCAP modulated the pyloric pattern in *stn*-intact *L. emarginata* preparations. **A)** The LP neuron's burst duration decreased in the presence of CCAP (n=15, paired t-test: p=0.0496). **B)** PD neurons' spike frequency decreased after CCAP application (n=15, paired t-test: p=0.0007). **C)** The IC neuron burst duration decreased in the presence of CCAP (n=10, paired t-test: p=0.0022). **D)** The duty cycle of the IC neuron decreased in the presence of CCAP (n=10, paired t-test: p=0.0291). **E)** IC neuron spike frequency increased after CCAP application (n=10, paired t-test: p=0.0081). **F)** VD neurons exhibited an increased spike frequency during CCAP application (n=4, paired t-test: p=0.0024). * = $p \leq 0.05$; ** = $p \leq 0.01$; *** = $p \leq 0.001$

Oxotremorine–L. emarginata

The muscarinic acetylcholine agonist oxotremorine modulated the pyloric pattern in all eight *stn*-intact *L. emarginata* preparations to which it was applied. No net cycle period alterations were observed during oxotremorine application. The duty cycle of the LP neuron increased during oxotremorine application (Fig. 23A, n=8, paired t-test: p=0.0068), but no other LP firing parameters were affected. The duty cycle of PY neurons decreased (Fig. 23B, n=7, paired t-test: p=0.0032) and their spike frequency increased (Fig. 23C, n=7, p=0.0173), but oxotremorine had no effect on PY neuron burst duration. PD neurons exhibited an increase in burst duration (Fig. 23D, n=8, p=0.0078) during proctolin application. No other PD neuronal firing characteristics were altered by oxotremorine. VD and IC neurons were recorded in the presence of oxotremorine, but no significant alterations to their firing statistics were observed.

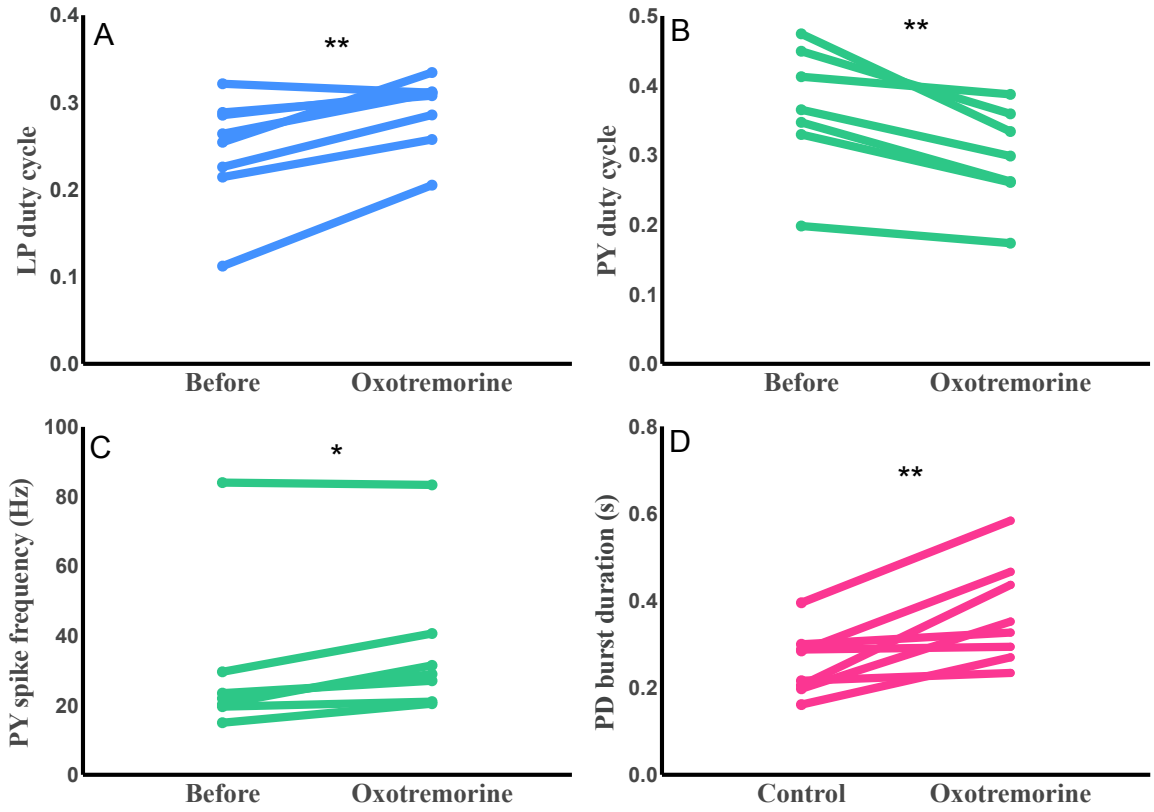

Figure 23. Oxotremorine modulated the pyloric pattern in *stn*-intact preparations of *L. emarginata*. **A)** LP duty cycle increased in the presence of oxotremorine (n=8, paired t-test: p=0.0068). **B)** PY duty cycle decreased during oxotremorine application (n=7, paired t-test: p=0.0032). **C)** PY spike frequency increased in the presence of oxotremorine (n=7, paired t-test: p=0.0173). **D)** Burst duration of PD neurons increased during oxotremorine application (n=8, paired t-test: p= 0.0078). * = $p \leq 0.05$; ** = $p \leq 0.01$

Transcriptome assembly for C. opilio tissues

To determine whether differential receptor expression might be a mechanism underlying differential modulatory capacity in the STNS, total RNA samples were obtained from *C. opilio* males to be sequenced for transcriptome assembly. RNA from six pairs of eyestalks (concentrations range from 21.8-130.0 ng/µl) and six brains (21.1-66.8 ng/µl) was isolated (Table 1). All samples were deemed to be high quality by Agilent Tapestation electropherogram and gel electrophoresis. Illumina RNA-seq yielded 42.8 - 62.3 million reads for brain samples and 48.0 – 63.8 million reads for eyestalk samples (Table 1).

Table 1. Concentrations of total RNA isolated from male *Chionoecetes opilio* tissue to be used in transcriptome assembly and paired-ended RNA-seq raw read counts. All samples were collected from male animals. B=brain; E=eyestalk

Sample ID	Total RNA concentration (ng/µl)	RNA-seq raw read count (forward and reverse)
B2	21.1	48,383,126
B3	66.8	48,936,774
B4	66.2	42,853,350
B6	57.5	57,532,290
B7	27.6	62,295,755
B8	43.9	50,904,257
E2	21.8	53,522,043
E3	130.0	63,766,985
E5	98.6	48,041,775
E6	73.5	55,518,469
E7	48.7	45,019,017
E8	103	54,283,269

Using Trinity software, we successfully *de novo* assembled two *C. opilio* transcriptomes, one specific to brain tissue and the other to eyestalk ganglia tissue. The observed number of assembled contigs was much higher than seen in previous assemblies of crustacean transcriptomes, 1,174,280 contigs for brain tissue and 1,321,304 contigs for eyestalk ganglia tissue. This in turn created a vast number of Trinity 'genes,' 662,415 for brain tissue and 727,705 for eyestalk ganglia tissue (Table 2). In hopes of decreasing the likely high level of redundancy in each transcriptome, similar sequences were clustered using CD-HIT-EST. This reduced both

the number of total contigs, to 824,736 for the brain transcriptome and to 912,813 for the eyestalk transcriptome, and the number of Trinity 'genes' to 634,067 for the brain transcriptome and to 693,879 for the eyestalk transcriptome (Table 2).

Table 2. Assembly statistics for a *C. opilio* brain and eyestalk ganglia tissue-specific transcriptome assemblies using Trinity (v2.8.4) after adapter trimming (Grabherr et al., 2011). Assembly statistics were gathered using the Trinity Toolkit script Trinitystats.pl and sequence analysis information from CD-HIT. Transcriptome statistics after expressed sequence tag clustering through CD-HIT-EST, performed to reduce transcript redundancy, are given in columns labelled "clstr." Abbreviations: bp, base pairs; clstr, clustered; GC, guanine-cytosine.

Assembly statistic	Brain transcriptome	Brain transcriptome (clstr)	Eyestalk ganglia transcriptome	Eyestalk ganglia (clstr)
Total number of bases assembled	708,584,927	453,669,282	800,520,201	509,118,657
Total number of assembled contigs	1,174,280	824,736	1,321,304	912,813
Total number of Trinity 'genes'	662,415	634,067	727,705	693,879
N10 (bp)	4,186	3,169	4,009	3,093
N20 (bp)	2,301	1,615	2,205	1,606
N30 (bp)	1,388	1,051	1,360	1,061
N40 (bp)	950	781	944	795
N50 (bp)	709	615	710	627
Shortest contig length (bp)	169	173	170	177
Longest contig length (bp)	32,678	32,678	42,134	42,134
Median contig length (bp)	390	381	395	388
Average contig length (bp)	603.42	550.08	605.86	557.75
GC content (%)	43.54	42.89	43.40	42.82

Although CD-HIT-EST was able to reduce the number of contigs in each transcriptome, additional exploratory analysis was performed to determine the nature of these large

transcriptomes. Two iterations of a BUSCO analysis were performed on each transcriptome. This analysis protocol employs BLAST software to mine transcriptomes for around 1,000 coding genes that should be present in the transcriptome, taking phylogeny into account (Seppey et al., 2019). It should be noted that these genes are not specific to neuronal tissue, but should be present as a single copy in all cell types. The analysis was run on each transcriptome, prior to CD-HIT clustering in 'transcriptome mode.' Out of the total 1,013 BUSCO gene queries, results are broken down by those genes which are complete (C) and single-copy (S) or duplicated (D), fragmented (F), or missing (M) (Fig. 24). For the brain transcriptome, 93.2% of transcripts corresponding to BUSCO genes were found in their complete form. Of these, 34.3% were found once and 58.9% were duplicated one or more times. A small percentage of transcripts, 1.3%, were fragmented versions of the BUSCO genes and 5.5% of BUSCO genes were not found in the transcriptome. For the eyestalk transcriptome, 32.8% of BUSCO genes were found in their complete form once and 61.0% of BUSCO genes were found in duplicate. As in the brain transcriptome, a small number of BUSCO genes, 1.5% were only found as fragments and 4.7% of BUSCO genes were not found.

A separate BUSCO analysis was performed in 'protein mode' after translating each transcriptome into peptide sequences through TransDecoder by the longest open reading frame. This yielded slightly different results than when BUSCO analyses were run on the raw transcriptomes. For the brain translated-transcriptome, 34.8% of BUSCO proteins were found once and 61.3% were found in duplicate, 1.8% were found as fragments, and 2.1% of BUSCO proteins were not found. In the eyestalk transcriptome, 33.7% of BUSCO proteins were found as single-copies and 63.2% were found to be duplicated, 1.5% of genes were found as fragments, and 1.6% of BUSCO proteins were not found.

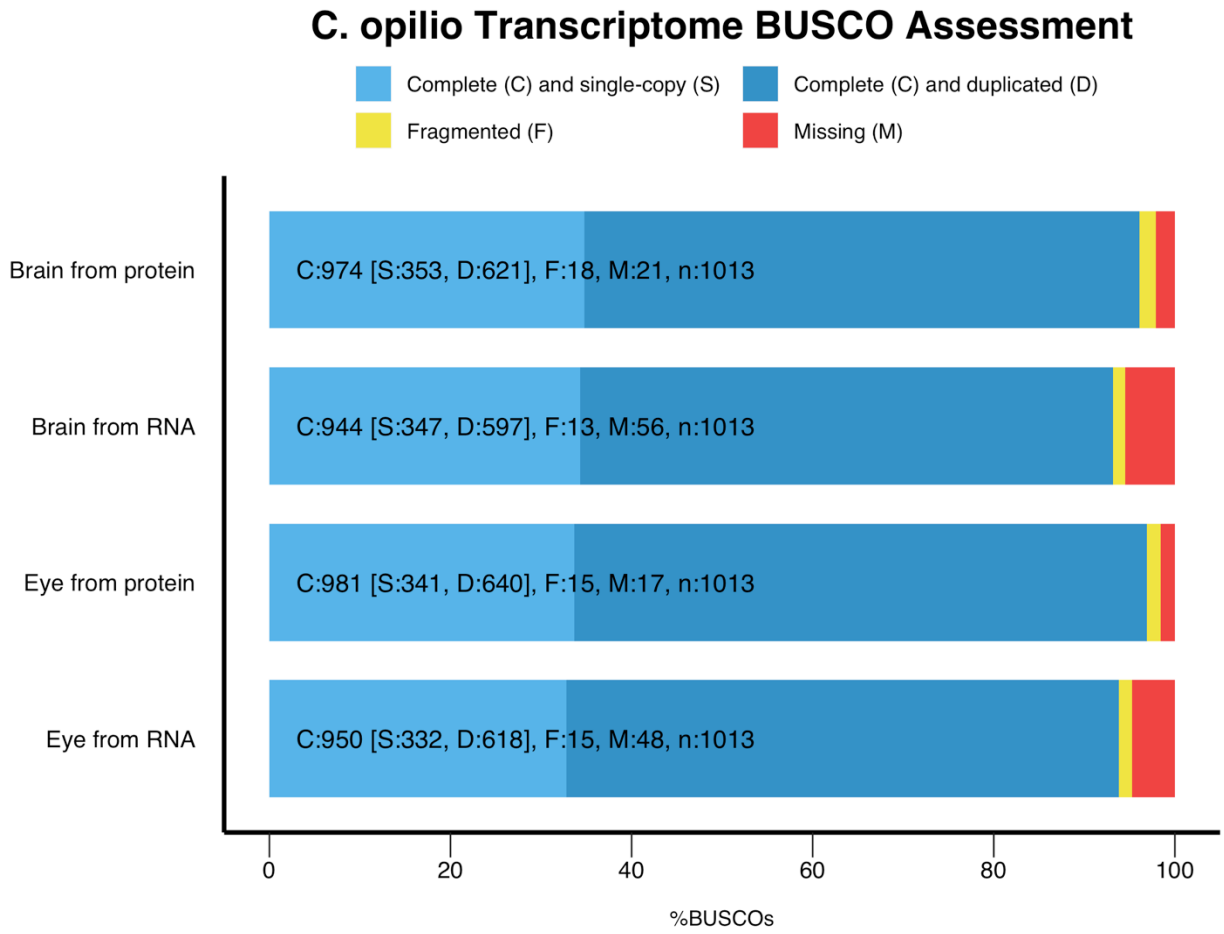

Figure 24. BUSCO assessment summaries for brain and eyestalk ganglia transcriptomes from *C. opilio*. The analysis was performed using a set of 1,013 genes which are highly conserved among arthropod species (Seppey et al., 2019). Two iterations of the analysis were performed for each transcriptome. First, the analysis was performed in 'transcriptome mode,' searching for transcripts in the raw transcriptome file (indicated in figure as "from RNA"). Second, the transcripts were translated into peptide sequences through an open reading frame method by TransDecoder (reviewed in Haas et al., 2013), and a BUSCO analysis was performed in 'protein mode' on the translated transcriptome (indicated in figure as "from protein"). For each of the four BUSCO analyses, values are provided for the presence of transcripts or peptide sequences which are: complete (C) and single-copy (S) or duplicated (D), fragmented (F), or missing (M).

In order to investigate possible sources of the uncharacteristically large number of contigs and Trinity 'genes' present in the two *C. opilio* transcriptomes, an abundance analysis was performed. Based on the relative expression parameter transcripts per million (TPM), transcripts

expressed higher than 1.00 TPM were excluded as outliers, reducing the brain transcriptome by 7.35% and the eyestalk ganglia transcriptome by 7.90%. The remaining transcripts show a strong right skew with the highest number of transcriptomes falling between 0.09 and 0.12 TPM in both transcriptomes (Fig. 25).

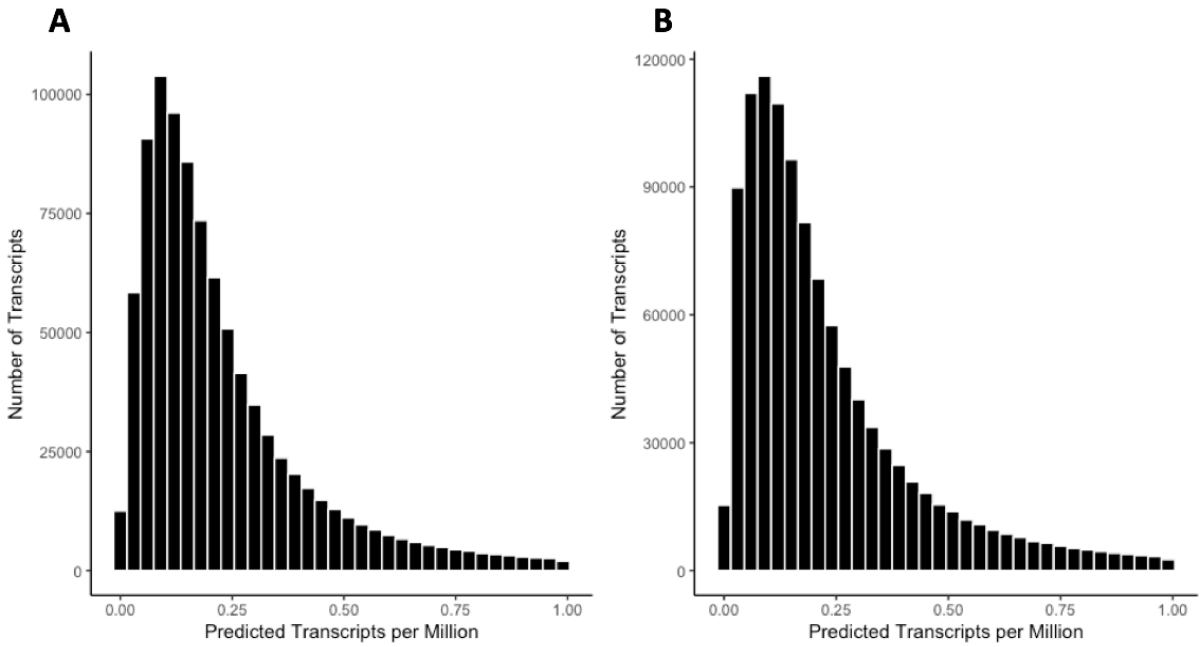

Figure 25. Distribution of lowly expressed transcripts in brain and eyestalk ganglia transcriptomes of *C. opilio*. Relative transcript abundances were averaged across samples to show average distributions. Transcripts greater than 1.00 transcripts per million (TPM) were removed in order to visualize transcripts with low expression levels. The majority of transcripts fall below 0.25 TPM. **A)** Distribution of relative transcript abundance in brain tissue. **B)** Relative transcript abundances in eyestalk ganglia tissue.

Predicted neuropeptidome for the Majoidea superfamily

Using BLAST software, previously assembled transcriptomes for the brain and the stomatogastric ganglion of *Pugettia producta* and *Libinia emarginata,* as well as the currently assembled brain and eyestalk ganglia transcriptomes of *C. opilio,* were mined. A variety of neuropeptides, including those tested on preparations in this study and future modulators to be used in physiological studies were mined for. These results are summarized below (Table 3). Interestingly, no BLAST hits were returned in any of the *L. emarginata, P. producta,* or *C. opilio*

transcriptomes for the entire FMRFamide-like peptide family. FMRFamide-like peptide sequences were found in the two *C. opilio* transcriptomes using different query methods, and these results are given below. Annotated prepro sequences are given for those peptides which were found in a respective transcriptome, verified as a signal protein, and confirmed through sequence homology with both *Drosophila melanogaster* and a related crustacean species (Fig. 26). Note that splice variants and minor isoforms are not shown.

Table 3. Mining results for the existence of various neuropeptides in members of the Majoidea superfamily. Peptide families and subsequent peptides within a single family that were mined for are listed. For those crab species in which evidence of a particular peptide was found (signified by a check mark), a tblastn search statistic (raw score) and E-value are given. An 'X' indicates no returned hit through tblastn. Abbreviations: CCAP, crustacean cardioactive peptide; DH, diuretic hormone; FLP, FMRFamide-like peptide; RPCH, red pigment concentrating hormone.

Peptide family	Deduced protein	*L. emarginata brain*	*L. emarginata STG*	*P. producta brain*	*P. producta STG*	*C. opilio brain*	*C. opilio eyestalk*
CCAP	Prepro-CCAP	✓ (93, 2e-3)	X	X	✓(91, 3e-3)	✓ (99, 3e-4)	✓(99, 4e-4)
CCH	Prepro-CCHamide I	✓(172, 9e-13)	X	✓(180, 1e-13)	X	✓(200, 7e-19)	✓(200, 2e-18)
DH31	Prepro-DH31	✓(153, 1e-10)	✓(153, 3e-75)	✓(153, 1e-10)	✓(153, 4e-74)	✓(139, 1e-12)	✓(152, 6e-13)
FLP	GYSDRNYLRF amide	X	X	X	X	X	X
	SGRNFLRF amide	X	X	X	X	X	X
	NRNFLRFamide	X	X	X	X	X	X
	DQNRNFLRF amide	X	X	X	X	X	X
	GAHKNYLRF amide	X	X	X	X	X	X
	GNRNFLRF amide	X	X	X	X	X	X
	GDRNFLRF amide	X	X	X	X	X	X
	FSHDRNFLRF amide	X	X	X	X	X	X
	APSKNFLRF amide	X	X	X	X	X	X
FLRFamide	Myosuppressin	✓(303, 6e-28)	X	✓(283, 1e-25)	X	✓(280, 2e-31)	✓(281, 1e-31)
Proctolin	Prepro-proctolin	✓(152, 2e-10)	✓(152, 1e-10)	✓(157, 5e-11)	✓(157, 4e-11)	✓(143, 7e-11)	✓(143, 5e-11)
RPCH	Prepro-RPCH	✓(236, 3e-20)	X	✓(241, 8e-21)	X	✓(202, 4e-19)	✓(203, 6e-20)

The existence of transcripts for each peptide appeared to vary between each organism and its respective tissues. A putative prepro-sequence for CCAP isoform A was identified in the brain of *L. emarginata* (142 amino acid residues, Fig. 26A), the STG of *P. producta* (140 amino

acid residues, Fig. 26A1), and in both *C. opilio* transcriptomes (143 amino acid residues, Fig. 26A2), with homology confirmed through *D. melanogaster* (FlyBase ID: FBpp0307015). These three sequences are highly similar (69.5-85.9% identity), with slight variances only in the signal peptide sequence and some linker peptide sequences. Interestingly, no valid hits for CCAP isoform A were found during BLAST analysis of the *L. emarginata* STG. For the brain of *P. producta*, a 19 amino acid coding sequence was deduced, but was not determined to contain any part of a signal peptide sequence. Therefore, this may be a partial C-terminus fragment of the CCAP isoform A sequence, but it did not overlap with the CCAP isoform A sequence from the STG of the same species.

Putative precursor proteins for CCHamide I were deduced from the *L. emarginata* brain transcript (122 residues, Fig. 26B) and the *P. producta* brain transcript (121 residues, Fig. 26B1), and in both *C. opilio* transcriptomes (123 residues, Fig. 26B2). In these sequences, the active peptide sequence for which the peptide is named comes directly after the N-terminus of the signal sequence. Identities for the full length of the prepro peptide between the three species were relatively high, between 66.8% and 95.4%. These active peptide sequences are nearly identical, save for a glutamate and glycine pair that is considered part of the signal sequence for the peptide deduced from *P. producta* brain and the *C. opilio* transcriptomes, but is considered part of the active peptide sequence for the peptide deduced from *L. emarginata* brain, which was determined by SignalP. As with CCAP, there are slight differences between the two sequences in both the signal sequence and the linker/precursor sequences. For the STG of *L. emarginata,* a transcript was identified from the tblastn algorithm (score: 69), but it was not determined to contain a signal sequence nor an active peptide sequence. Peptide homology analysis in both *D. melanogaster* and *Leptidea sinapis* (the wood white butterfly, an arthropod), returned

uncharacterized proteins and not CCHamide isoforms. Therefore, this was not considered a fragment of CCHamide I, although it may be an C-terminus linker peptide fragment. For the *P. producta* STG transcriptome, the tblastn protocol did not return any hits.

Prepro diuretic hormone 31 (DH31) sequences were deduced from both *P. producta* transcriptomes, from both *L. emarginata* transcriptomes, and from both *C. opilio* transcriptomes. The two transcriptomes of *L. emarginata* provided the same peptide sequence for DH31, consisting of 143 amino acids (Fig. 26C). The peptide sequence was identical in the brain and STG of *P. producta*, consisting of 142 amino acid residues (Fig. 26C1). The sequence was also identical in both *C. opilio* transcriptomes, and consisted of 141 amino acid residue (Fig. 26C2). Between the prepro sequences for DH31 in *P. producta* and *L. emarginata*, a 92.3% sequence identity was observed; a 75.5% sequence identity was found between *L. emarginata* and *C. opilio;* and a 77.4% sequence identity was found between *C. opilio* and *P. producta*. In the *L. emarginata* and *P. producta*, the sequences of the active region are identical and contain four linker sequences, which have slight differences. However, the active region sequence differs in *C. opilio* with a serine at residue 83, as opposed to a threonine residue in *L. emarginata* and *P. producta* at this site. Additionally, the arginine at residue 32 was not determined to be a cleavage site in *C. opilio*, but was in the other two species, resulting in only three linker sequences in this prepro-peptide. Based on homology with *H. americanus*, the glycine residue at the C-terminus of the active peptide sequence is likely amidated (Christie et al., 2017).

Similarly to DH31, putative sequences for the proctolin precursor were identical in the brain and STG of *L. emarginata*, identical in the brain and STG of *P. producta*, and identical in the brain and eyestalk of *C. opilio*. In *L. emarginata* tissues, the dominant prepro-proctolin sequence consists of 91 residues with four linker sequences (Fig. 26D). In *P. producta* tissues,

the sequence consists of 93 amino acids with five linker sequences (Fig. 26D1). In *C. opilio* tissues, the sequence is 94 amino acids long with five linker sequences. Between the three species, the active peptide sequence, RYLPT, is conserved and sequence identities for the entire prerpo-peptide vary between 75.4% and 84.9%. Minor alterations in the signal sequence and linker/precursor sequences were observed between the species, although there are no major differences. The phylogenetically closest sequence within the arthropod phylum from reciprocal BLASTing in NCBI BLAST was shown to be Nephrops norvegicus (Norway lobster, NCBI txid: 6829) for all three species.

A putative precursor peptide sequence for RPCH was found in the brain transcriptomes of *L. emarginata* (Fig. 26E) and *P. producta* (Fig. 26E1), and in both *C. opilio* transcriptomes (Fig. 26E2). In all three species, the deduced prepro-RPCH sequence was 108 amino acids long and contained 2 linker sequences. Sequence identities between the three species varied between 88.9% and 95.4% for the whole prepro-RPCH sequence. The active peptide regions of these sequences are identical and have an amidated glycine residue on the C-terminus end. There are slight alterations between the each species' exact sequences in both the signal and linker regions. The active peptide sequence for RPCH (QLNFSPGWamide) seems to be conserved within crustaceans, as studies of *H. americanus* report the identical sequence (Christie et al., 2017; Ma et al., 2008; Stemmler et al., 2006). Interestingly, no hits were returned from the tblastn protocol in the transcriptome from STG tissues of *L. emarginata* and *P. producta*.

Putative prepro-myosuppressin sequences were found in the brain transcriptome of *L. emarginata* (Fig. 26F), the brain transcriptome of *P. producta* (Fig. 26F1), and in both *C. opilio* transcriptomes (Fig. 26F2). In *L. emarginata* and *C. opilio*, the deduced sequences are 100 amino acid residues long, with 93.0% identity between them. In *P. producta,* the sequence is 101 amino

acid residues long, sharing a 90.1% identity with *C. opilio* and a 93.1% identity with *L. emarginata.* In all three species, the active peptide region is identical with the sequence QDLDHVFLRFG. As in *H. americanus,* the glutamine residue at the N-terminus end of the active peptide sequence likely exists as pyroglutamic acid and the glycine resiude at the C-terminus site is amidated. All three deduced sequences contain three linker peptides, with the C-terminus linker sequence consisting of only three amino acid residues. No hits were returned by tblastn for the STG transcriptomes of *P. producta* and *L. emarginata*.

Using a direct search method on the two *C. opilio* transcriptomes after translation with TransDecoder, multiple FMRFamide-like peptides (FLPs) were discovered. Only one of these peptides was identical to an FLP deduced from *H. americanus* eyestalk transcriptomes: NRNFLRFG. Five other FLPs were found in both tissues of *C. opilio*: AGRNFLRFG, AYNRSFLRFG, SPQRNFLRFG, DLFLRFG, GYNKNYLRFG. However, the homology of these sequences to other crustaceans or arthropods was not assessed.

A. Prepro-CCAP from *L. emarginata* brain

MAMTYTNWCRRAGLMSAGAFLVLVMMASNASAGPVS**KR**DIDGLLDGKL**KR**PFCNAFTGCG**KK**RS
DPELEGLASGSELDDLAKHVLAEARLWEGLQSKMEAMRLFAS**R**LDSRPTFR**RKR**FIDQHKDAYS
ASSTLNNKVDAEKQ

A1. Prepro-CCAP from *P. producta* STG

MTMTYTSWCRRAGLVSAAFLVLVLMASHATAGPVS**KR**DIDSLLDGKL**KR**PFCNAFTGCG**KK**RSD
PELEGLASGSELDDLAKHVLAEARLWEQLQGKMEAMRLLAS**R**MDSRPTF**RRKR**FIDHHQDDYSA
STLNHKEGSEKQ

A2. Prepro-CCAP from *C. opilio* brain and eyestalk (identical)

MKMTNTSWCARVGMVLASTVLLLVLLASNAQAGPVF**KR**DIDSLFDGKI**KR**PFCNAFTGCG**KK**RS
DPELEGLASGSELNDLAKHVLAEAKLWEQLQSKMEAMRSLAS**R**MDSGPMF**RRKR**YSNQQQHDDT
HSTQTLEYKGGAEKE

B. Prepro-CCHamide I from *L. emarginata* brain

MGRVVLSAVLCLVVASTFTSLAEGKCSQFGHSCFGAHG**KR**GGGDQYGGGLEPADLYPQNNQLPE
MDEARYPLDDATVTNPRNIAKVRDLMDIVGHLLRQRAGGIQQRPLPAAQLPPNDAYLH

B1. Prepro-CCHamide I from *P. producta* brain

MGRVAFSVVLCLVVASTFVSLAEGKCSQFGHSCFGAHG**KR**GGGDQYGGSLEPADLYPQSNQVPE
LDEARYPLDDAAVTNPRNIAKVRDLMDIVGHLLRQRAGNQQRPLPAAQLPPNDAYLH

B2. Prepro-CCHamide I from *C. opilio* brain and eyestalk (identical)

MGRVAFSVILCLGVASSVLKLAEGKCSQFGHSCFGAHG**KR**GGDQYGSLDPAALYPPSNQLAEER
FPLDEAPQPNLRAMAQARDLMDIVGHLLRQRAAIQQQQQQQQQPRPLAAQLGPNDAYLH

C. Prepro-DH31 from *L. emarginata* brain and STG (identical)

MNNLGVVFVSLVAAFVVLSSVNATPINRESS**R**AVVEVDDPDYVLELLTRFSNSII**R**AKELEKFT
RSSSGA**KR**GLDLGLGRGFTGSQAAKHLMGLAAANYAGGPG**RRKR**ESQAAPSDLLHDDLHAHEHD
AAAAAPAGLSLHSTR

C1. Prepro-DH31 from *P. producta* brain and STG (identical)

MNNLGVVFVSLVAAFVILSSVNATPINREPS**R**AVVEVDDPDYVLELLTRISNSII**R**AKELEKFT
RSSSAA**KR**GLDLGLGRGFTGSQAAKHLMGLAAANYAGGPG**RRKR**EAQAATPDLHQDDLPAHEHD
AAAAAAGLSLHSTR

C2. Prepro-DH31 from *C. opilio* brain (identical)

MNNLSVVLVSLAATVILLSSLHATPINREASRAVVEIDDPDYVLELLTRFTNSII**R**AKELEKFV
RSSNTA**KR**GLDLGLGRGFSGSQAAKHLMGLAAANYAGGPG**RRKR**DSEAATLDTHRDDFSAQEYE
TAANAGLPLPLSR

D. Prepro-proctolin from *L. emarginata* brain and STG (identical)

MARMGLLVVALVVMVVAEVTQARYLPT**R**ADDSRLEEI**R**ELLKELLERTAEGGVGSGNTSARLNY
E**KR**FLF**KR**AVPAGGADEVAQPLINLPQ

D1. Prepro-proctolin from *P. producta* brain and STG (identical)

MARVGLMVVVVALVVMVVAEVTQARYLPT**R**ADDSRLEEI**R**ELLREVLE**R**TAEGGVGSGNTSGRM
NYD**KR**FLF**KR**AAPMGGADEMAQPLINLPQ

D2. Prepro-proctolin from *C. opilio* brain and eyestalk (identical)

MARCGLLVVVVALVVVSAGVSQGRYLPT**R**ADDSRLDEI**R**ELLRALLE**R**TAEGGLGSGTANTSGR
LTYD**KR**FLF**KR**AAPVVGAGEVVEPLINLPQ

E. Prepro-RPCH from *L. emarginata* brain

MVRRAGVTPLVVALVVVALVSSVSAQLNFSPGWG**KR**AAAAGGSSGSVGEAVSALHSVAASPRGV
VPPGSSSSGDSCGPIPVSAVMHIYRLI**R**SEAMRLVQCQEEEYMG

E1. Prepro-RPCH from *P. producta* brain

MVRRAGVTLLVAALVVVALVSSVSAQLNFSPGWG**KR**AAAAGGNSGSVGEAVSALHSVAASPRGV
MPPGSSSSGDSCGPIPVSAVMHIYRLI**R**SEAMRLVQCQDEEYMG

E2. Prepro-RPCH from *C. opilio* brain and eyestalk (identical)
MVRGTGVTLLVAALVVVALVSSVSAQLNFSPGWG**KR**ASAAGGSSGGVGEAVSALHSVATSPRGV
VAPGSSSSGDACGPIPVTAVMHIYRLI**R**SEAMRLVQCQDEEYLG

F. Prepro-myosuppressin from *L. emarginata* brain
MVFRLQPWCSLLVVGVVVMLGVCTGVGEAIPPPICYNQKLVLSPYA**RR**LCAALSDISRFSGAME
EYLDAQAIKNSMGVNEPEV**KR**QDLDHVFLRFG**R**AQL

F1. Prepro-myosuppressin from *P. producta* brain
MVFRLQPWCSLVVVGVVVMLGACAGVGEAIPPPPICFNQKLVLSPYA**RR**LCAALNDISRFSGAM
EEFLDAQAIKNSMGVNEPEV**KR**QDLDHVFLRFG**R**AQL

F2. Prepro-myosuppressin from *C. opilio* brain and eyestalk (identical)
MVFRLQPWCSLLLVGVVVVLGVCAGVGEAIPPPICFNQKLSLSPYA**RR**LCAALSDISKFSGAME
DYLDAQAIKNSMGVNEPEV**KR**QDLDHVFLRFG**R**AQL

Figure 26. Putative prepro-peptide sequences for signaling peptides in members of the Majoidea superfamily. Only dominant isoforms are shown, with splice variants and minor isoforms not provided. **A)** Prepro-crustacean cardioactive peptide A deduced from the *L. emarginata* brain transcriptome. **A1)** Prepro-crustacean cardioactive peptide A deduced from the *P. producta* STG transcriptome. **A2)** Prepro-crustacean cardioactive peptide A deduced from *C. opilio* brain and eyestalk transcriptomes. **B)** Prepro-CCHamide I deduced from the *L. emarginata* brain transcriptome. **B1)** Prepro-CCHamide I deduced from the *P. producta* brain transcriptome. **B2)** Prepro-CCHamide I deduced from *C. opilio* brain and eyestalk transcriptomes. **C)** Identical prepro-diuretic hormone 31 sequences from the *L. emarginata* brain and STG transcriptome. **C1)** Identical prepro-diuretic hormone 31 from *P. producta* brain and STG transcriptomes. **C2)** Prepro-diuretic hormone 31 sequences, identical from *C. opilio* brain and eyestalk transcriptomes. **D)** Identical prepro-proctolin sequences from *L. emarginata* brain and STG transcriptomes. **D1)** Identical deduced prepro-proctolin peptide sequences from *P. producta* brain and STG. **D2)** Identical prepro-proctolin sequences deduced from *C. opilio* brain and eyestalk transcriptomes. **E)** Prepro-RPCH from the *L. emarginata* brain transcriptome. **E1)** Prepro-RPCH from the *P. producta* brain transcriptome **E2)** Identical prepro red pigment concentrating hormone sequence deduced from *C. opilio* brain and eyestalk transcriptomes. Signal peptide sequences, deduced from SignalP (v5.0) are shown in grey for each sequence. The active peptide sequence for which the protein is named is shown in red, while linker and precursor proteins are shown in blue. Mono and dibasic cleavage sites are shown in bold black.

DISCUSSION

Our underlying hypothesis was that neuromodulation is a substrate for the evolution of behavioral diversity. In the case of the STNS, a variety in neuromodulation can enable a certain degree of flexibility in rhythmic motor outputs. The need for behavioral diversity, or the ability to digest various foods, was expected to be correlated with modulatory capacity. As a species that subsists on one food source, *Pugettia producta* does not need flexibility in stomach muscle movements to break down different foods. On the other hand, opportunistic feeders such as *Libinia emarginata* and *Chionoecetes opilio* consume many types of food in their environment, and require highly diverse digestive muscle movements to mechanically break down and filter these different foods. Therefore, we predicted that the opportunistic feeder *C. opilio* should possess a wider neuromodulatory capacity than has been previously reported in the specialist feeder *P. producta* (Dickinson et al., 2008). Rather, we expected the modulatory capacity of *C. opilio* to be similar to that of the opportunistic feeders *Cancer borealis* and Majoidea superfamily member *L. emarginata* (Miller, 2018).

Modulation of the pyloric pattern in the Majoidea superfamily

These preliminary data from the *C. opilio* STNS suggest that the snow crab STNS is responsive to the full suite of neuromodulators tested in this study: CabTRP Ia (n=1, Fig. 3, Fig. 4), RPCH (n=3, Fig. 6), proctolin (n=2, Fig. 9), CCAP (n=4, Fig. 12), dopamine (n=1, Fig. 14, Fig. 15), oxotremorine (n=1, Fig. 16, Fig. 17), and myosuppressin (n=4, Fig. 18). Although these changes in firing characteristics are not significant, each modulator appeared to impact the pyloric pattern qualitatively during application. This is congruent with the opportunistic feeders *L. emarginata* and *C. borealis*, and contrary to *P. producta* (Table 4). This further supports the hypothesis that the differences in modulatory capacity within the order Decapoda are a result of

diet, rather than a product of phylogenetic distance. However, these conclusions are based on small sample sizes and significance testing could not be performed for all modulators.

Similar to the *C. opilio* physiological results, pooled data from isolated *stn*-intact preparations show that the pyloric pattern of *L. emarginata* is modulated by the five neuromodulators tested in this study: CabTRP Ia (n=15, Fig. 19), RPCH (n=13, Fig. 20), proctolin (n=10, Fig. 21), CCAP (n=15, Fig. 22), and oxotremorine (n=8, Fig. 23). Taken with previous data from the Dickinson lab examining the modulatory effects of dopamine and myosuppressin on the pyloric pattern of *L. emarginata,* we can conclude that the STNS of this organism is responsive to the full suite of neuromodulators used in this study. Again, this is in contrast to the specialist *P. producta*, which shows a narrower modulatory capacity, but in agreement with the opportunistic feeders *C. borealis* and *C. opilio.* However, the effects of each modulator on preparations of *L. emarginata* and *C. opilio* differ, with some differing from reported results in *C. borealis.*

Table 4. Summary of modulator effects in isolated STNS preparations of *Cancer borealis, Pugettia producta, Libinia emarginata,* and *Chionoecetes opilio*. A '+' indicates modulation by the specific modulator, a '–' indicates no modulation. Inconsistent modulation in *P. producta* is indicated parenthetically. Adapted from (Blitz et al., 2008; Dickinson et al., 2008; Harris-Warrick et al., 1992; Hui et al., 2011; Miller, 2018; Norris et al., 1994; Nusbaum and Marder, 1988; Nusbaum and Marder, 1989; Weimann et al., 1997).

Modulator	*Cancer borealis*	*Pugettia producta*	*Libinia emarginata*	*Chionoecetes opilio* (preliminary)
RPCH	+	+ (<25% of preparations)	+	+
CabTRP Ia	+	–	+	+
CCAP	+	–	+	+
Proctolin	+	+	+	+
Myosuppressin	+	+ (preliminary)	+	+
Dopamine	+	+ (inconsistent)	+	+
Oxotremorine	+	+	+	+

CabTRP Ia is a highly conserved signaling peptide in majoid crabs, released into the STNS from the post-oesophageal commisures, and affecting both the pyloric and gastric mill patterns (Blitz et al., 2008; Christie et al., 1997). In *C. borealis,* CabTRP Ia can activate the pyloric pattern if the pattern is not active, as well as reduce the cycle period of the whole pattern if the pattern is active (Hui et al., 2011). In *P. producta,* CabTRP Ia has been shown to have no effect on the pyloric pattern in either *stn*-cut or -intact preparations (Dickinson et al., 2008). In this study, CabTRP Ia modulated the pyloric rhythm of *C. opilio* by increasing PD and VD spike frequency during bursts, and by decreasing the spike frequency of LP and PY neurons. However, this is based on a single STNS preparation. In *L. emarginata*, application of CabTRP Ia resulted in an increase in spike frequency during bursts for both IC and LP neurons, as well as a decrease

in the duty cycle of PY and PD neurons (Fig. 19). No significant effects on cycle period were seen in either species, incongruent with data from *C. borealis*. Since modulation by CabTRP Ia was seen seen in both *C. opilio* and *L. emarginata,* two opportunistic feeders, and has not been observed in the specialist *P. producta*, the hypothesis that a differential modulatory capacity is a product of diet diversity rather than phylogeny is supported.

RPCH is a hormone that was originally characterized as a regulator of pigment migration in crustacean species (Perkins and Snook, 1931). Applications of synthetic RPCH in *C. borealis* STNS preparations increase the cycle period of the pyloric pattern and can activate the pattern in *stn*-cut preparations (Nusbaum and Marder, 1988). In *C. opilio*, RPCH slightly increased cycle period and activated the full pyloric pattern in one blocked preparation (Fig. 7). Additionally, RPCH application increased the LP neuron's burst duration in two out of three preparations, and increased this neuron's spike frequency in all three preparations. Additionally, it increased the burst duration of PD neurons in one preparation and decreased it in another (Fig. 6) In *L. emarginata,* RPCH application decreased the cycle period of the pyloric rhythm, in contrast to *C. borealis*. PY spike frequency, LP burst duration, LP duty cycle, and IC spike frequency all increased in response to RPCH application in *L. emarginata* preparations (Fig. 20). In *P. producta, stn*-intact preparations show no response to RPCH application but in less than 25% of *stn*-cut preparations,u the pyloric pattern is activated (Dickinson et al., 2008). Although there is some responsiveness of *P. producta* STNS preparations to RPCH application, both *L. emarginata* and *C. opilio* exhibited a much more robust modulation by RPCH. Therefore, RPCH's modulatory effects support the hypothesis that diet diversity is a predictor of modulatory capacity.

Proctolin has been shown to modulate the pyloric pattern of *C. borealis* by decreasing the cycle period, increasing LP spike frequency and duty cycle, increasing VD spike frequency, and increasing IC duty cycle (Hooper and Marder, 1987; Nusbaum and Marder, 1989). In *P. producta*, proctolin modulates the pyloric pattern by increasing the burst duration of LP and IC, while also decreasing the interval between LP and PY bursting phases (Dickinson et al., 2008). In *stn*-cut preparations, proctolin is able to initiate the pyloric pattern in approximately half of preparations (Dickinson et al., 2008). In *C. opilio*, proctolin application had differing effects on cycle period between preparations, but increased the LP neuron's burst duration and spike frequency as noted in *C. borealis and P. producta* (Fig. 9). Unlike in these two species, the duration of the PD neurons' bursting increased after proctolin application in *C. opilio*. Proctolin application had differing effects on burst duration of PY neurons in *C. opilio*. In *L. emarginata*, proctolin increased the burst duration and duty cycle of LP neurons, increased the spike frequency and duty cycle of IC neurons, and increased the spike frequency of PY neurons. Additionally, PY duty cycle decreased in *L. emarginata* after proctolin application. These data show that proctolin is a robust modulator of *C. borealis, L. emarginata, C. opilio* and *P. producta.* This indicates that proctolin modulates members of the Majoidea superfamily regardless of diet diversity.

CCAP is another conserved secretory neuropeptide, which is released from pericardial organs into the hemolymph (Christie et al., 1995). In *C. borealis*, CCAP has been shown to activate the pyloric pattern in *stn*-cut preparations. In *stn*-intact preparations, CCAP can shift bursting of pyloric neurons to become out of phase, as well as decrease the cycle period of the pattern and increase LP burst duration (Weimann et al., 1997). In *C. opilio*, CCAP increased cycle period and the burst duration of both PD and PY neurons (Fig. 12). The burst duration of

the LP neuron increased in two preparations and decreased in two preparations in *C. opilio* after CCAP application. In *L. emarginata,* CCAP robustly modulated the pyloric pattern of *stn*-intact preparations by decreasing burst duration of LP and IC neurons, decreasing the spike frequency of PD neurons, decreasing the duty cycle of IC neurons, and increasing the spike frequency of both IC and VD neurons. CCAP modulates the pyloric pattern of opportunistic feeders (*C. borealis, L. emarginata,* and *C. opilio*) but has no effect on the pyloric pattern of *P. producta (Dickinson et al., 2008).* Therefore, differential modulation by CCAP supports the theory that modulatory ability is connected to diet diversity.

Dopamine is a highly conserved neuromodulator present in most animals with a central nervous system. In *C. borealis*, IC, LP, and PY neurons exhibit an increase in activity, but PD activity decreases during dopamine application (Harris-Warrick et al., 1992). In *stn*-intact *P. producta* preparations, dopamine yields inconsistent effects on the pyloric pattern. However, in *stn*-cut preparations of the *P. producta* STNS, dopamine activated the pyloric pattern in 70% of preparations. Therefore, dopamine is considered an inconsistent modulator of the pyloric pattern in *P. producta.* In *C. opilio*, dopamine modulated the pyloric pattern by increasing the burst durations of LP and VD, and by decreasing the burst duration in PD and PY neurons (Fig. 14, Fig. 15). Although the effects of dopamine on *L. emarginata* were not analyzed in this study, previous studies have shown that dopamine increases the duty cycle of PD neurons and decreases the duty cycle of PY neurons (Miller, 2018). Since dopamine appears to modulate the pyloric pattern in *C. borealis, P. producta, C. opilio,* and *L. emarginata*, this modulator seems to affect members of the Majoidea superfamily similarly.

Oxotremorine is a muscarinic acetylcholine receptor agonist, and was used in this study as a proxy for acetylcholine. The pyloric pattern effects of oxotremorine are not well

characterized in *C. borealis*, but the gastric mill pattern has been shown to be modulated by oxotremorine. Additionally, VD and IC activity decreases when this modulator is applied (Norris et al., 1994). In response to oxotremorine application, the cycle period of the *P. producta* pyloric pattern decreases, and the burst duration of PY neurons decreases. Oxotremorine was only successfully applied to one *stn*-intact *C. opilio* preparation, in which the spike frequency of PD neurons increased as did all burst statistics for the VD neuron (Fig. 14). In 75% of blocked preparations of the *C. opilio* STNS, oxotremorine application activated the pyloric pattern (Fig. 15). In *L. emarginata*, oxotremorine increased the burst duration of PD neurons, increased the duty cycle in LP neurons, increased the spike frequency and decreased the duty cycle of PY neurons (Fig. 23). Oxotremorine modulates the pyloric pattern in all of the Majoidea superfamily members, and is therefore considered to modulate independently of diet diversity.

Myosuppressin is a FLRFamide peptide that is highly conserved among decapod crustaceans. In *C. borealis*, myosuppressin application decreases the duty cycle and spike frequency of PD neurons, and decreases spike frequency in PY neurons (Miller, 2018). In *stn*-intact preparations of *L. emarginata*, myosuppressin significantly decreased the spike frequency in PY neurons. Myosuppressin completely eliminated the pyloric pattern in three of four *stn*-cut preparations of *L. emarginata* (Miller, 2018). Currently, studies of the effects of myosuppressin on the pyloric pattern in *P. producta* are underway. In three out of four s*tn*-intact *C. opilio* preparations, application of myosuppressin permanently eliminated the pyloric pattern (Fig. 18). Since data have not been published on the effects of myosuppressin in *P. producta*, it is unclear whether its modulatory effects differ with respect to diet diversity.

Assembly of a tissue-specific transcriptome for C. opilio

Physiological data strongly suggest that differential modulatory capacities are connected to diet diversity, but the mechanism of a differential modulatory capacity remains in question. We hypothesized that the expression of receptors for modulators that are ineffective in *P. producta* is lower in this organism's STG as compared to the STGs of *L. emarginata* and *C. opilio*. The goals of tissue-specific transcriptome assembly were twofold: to determine the sequences of modulators to be synthesized for physiological application and to determine the sequences for the respective modulator receptors. In future studies, these sequences can be employed to both expand the number of modulators applied during physiological recordings and to quantify the expression levels of their receptors through single ganglion qPCR, as described previously in *C. borealis* (Northcutt et al., 2019). We created two transcriptomes for *C. opilio*, one brain-tissue-specific and one eyestalk-tissue-specific, from isolated RNA for comparison with existing *L. emarginata* and *P. producta* transcriptomes. These two transcriptomes were successfully created; however, both show an uncharacteristically high number of transcripts and Trinity "genes" (Table 2). For example, the *C. opilio* eyestalk ganglia transcriptome yielded 662,415 suspected genes compared to 110,847 suspected genes from a similar transcriptomic analysis of *Homarus americanus* eyestalk ganglia (Christie et al., 2017). This may simply be a result of a deeper transcriptome assembly with more samples per transcriptome and the use of newer Illumina sequencing technology, as evidenced by the high number of raw RNA-seq reads (Table 1). Through such deep sequencing, rare and lowly expressed gene isoforms or splice variants may be sequenced. This may also be a function of the Trinity software, as it produces a single *De Bruijn* graph per transcript, determining splice variants and isoforms for each individually. The downstream grouping of these transcripts is highly conservative in Trinity, which may be a source of the large amount of Trinity 'genes' that were predicted (Cerveau and

Jackson, 2016). However, this high number of assembled contigs and suspected genes could also arise from an error in either the sequencing or assembly protocol; more exploratory analysis is required to determine the true cause of this difference.

In order to validate our hypothesis that the vast majority of sequences come from transcripts with low expression levels we performed an abundance analysis. The distribution of transcripts shows that in each transcriptome around 68% of transcripts are expressed less than 0.25 times per million (Fig. 25). However, the identities of these transcripts are not known. Exploratory analysis of the two transcriptomes show evidence of ribosomal RNA, which should have been completely extracted through the polyA selection protocol performed during sequencing. If the polyA selection failed, these transcriptomes may be contaminated with non-messenger sources of RNA. Additionally, these may be 'invented' transcripts, which are produced by Trinity in an attempt to capture possible permutations of contig joining.

To determine the completeness of transcriptome assembly, and to rule out possible sequencing or assembly errors, BUSCO gene analyses were performed. Overall, the results of the analyses indicated relatively complete transcriptomes, with 96.1% of BUSCO genes found in the translated version of the brain transcriptome and 96.9% of BUSCO genes found in the translated eyestalk transcriptome (Fig. 24). However, a majority of these genes were found in duplicate, roughly 60% in each transcriptome, whereas they should all be present as a single copy as determined by the BUSCO software (Seppey et al., 2019). Again, this may be a result of the Trinity software determining rare isoforms and splice variants to be separate genes. However, duplicate copies of BUSCO genes could potentially arise from sample contamination. The RNA samples used for RNA-seq were not collected in sterile environments, and a number of possible contaminants including human cells, bacterial cells in potentially infected crabs, and organisms

living on the carapaces of crabs may have entered sample solutions. Contamination could be potentially confirmed via a BLAST analysis of non-aligning transcripts in the non-redundant genome dataset in NCBI.

The around 4% of missing BUSCO genes can likely be explained by life cycle stage confounds and the impact of using a phylogenetic dataset on the scope of a phylum; in this case the arthropod dataset was used, which may not overlap perfectly with the genome of *C. opilio.* Additionally, BUSCO datasets are not specific to neuronal tissue. A similar tissue-specific transcriptome assembly performed with Trinity on the electric organ of *Tetronarce californica* found higher numbers of missing BUSCO genes (using eukaryote, metazoan, and vertebra lineage sets) than was found in this study, indicating that there may be a discrepancy in the predicted conservation of these genes in neuronal cell types (Stavrianakou et al., 2017). Without annotated genomes for these three species of Majoidea crabs, the relevance of these missing genes is unclear.

Interestingly, analyses run on translated transcriptomes yielded more complete copies of BUSCO genes than the analyses ran on the raw transcriptomes. Although the number of fragmented copies of BUSCO genes are relatively similar between the protein and transcript analyses, the number of BUSCO genes which were not found was greater for the RNA BUSCO analysis in both transcriptomes. One possible explanation for this discrepancy between the RNA analysis and protein analysis on the same set of transcripts arises from BUSCO's internal methods for identifying the existence of genes. During the analysis, the program builds statistical models dependent on the phylogenetic dataset to best predict the existence of these genes. Bogged down by the vast size of these transcriptomes, certain predictions made by the program in order to find some genes will inherently limit the ability of the program to find other genes

(Waterhouse et al., 2018). Once translated by TransDecoder, candidate reading frames have been identified and the overall size of the transcriptome is reduced. Therefore, more BUSCO genes can be easily identified by the program during protein analysis.

Mining transcriptomes to predict the neuropeptidome of the Majoidea superfamily

Determining the sequences of neuropeptides in each member of the Majoidea superfamily is crucial in understanding differences between the peptide structures across these three species, which may explain differences in modulator sensitivity. Additionally, by determining the sequences of neuropeptides that have not yet been analyzed, future studies may expand the number and variety of neuromodulators tested on the STNS of these three Majoidea species. The mining performed in this study only begins to describe the complex neuropeptidome of the Majoidea superfamily; however, some interesting results were derived.

In some cases, the sequences of neuropeptides were only found in a single tissue of an organism. CCAP was discovered in the brain of *L. emarginata*, the STG of *P. producta*, and in both the brain and eyestalk tissues of *C. opilio.* One possible explanation for the lack of CCAP expression in the *L. emarginata* STG transcriptome is that CCAP is known to be secreted from the pericardium into circulatory fluid (Christie et al., 1995). Therefore, transcription of this endocrine signal would not occur in the STG of *L. emarginata.* If this is due to a lack of transcriptome completeness, qPCR analysis of the *L. emarginata* STG may find that these transcripts do indeed exist. More puzzling is the existence of prepro-CCAP transcripts in the STG of *P. producta*. Physiological data from *P. producta* shows that CCAP does not modulate the pyloric pattern in this animal, and as stated above CCAP is not an autocrine or paracrine signal (Christie et al., 1995; Dickinson et al., 2008). More analysis is needed to determine the significance of CCAP in the *P. producta* STG.

Putative sequences for prepro-CCHamide I were found in the brains of both *L. emarginata* and *P. producta*, but not in the STG of either. The connection between physiological results and the inexistence of this peptide sequence from the STGs of these species is unclear. CCHamide I was found in both *C. opilio* transcriptomes. The active peptide sequence of prepro-CCHamide I differed between the species. In both *P. producta* and *C. opilio,* a glutamate and glycine pair exist at the N-terminus end of the signal sequence, but this pair is considered a part of the active peptide sequence in *L. emarginata*. This may have downstream consequences in the synthesis and application of CCHamide I to isolated STNS preparations.

For both diuretic hormone 31 and proctolin, prepro-peptide sequences were found in the brains and STGs of *L. emarginata* and *P. producta*, as well as in the brain and eyestalk tissues of *C. opilio*. In the case of DH31, there have been no studies of its effects on the pyloric pattern in decapod crustaceans. However, in *Drosophila melanogaster*, DH31 has been shown to modulate muscle contractions in the digestive tract (Vanderveken and O'Donnell, 2014). The active peptide sequence for DH31 differ between the species, with a serine at residue 83 in *C. opilio* and a threonine residue at this site in both *L. emarginata* and *P. producta*. Again, this may have consequences in the application of synthetic DH31 in STNS preparations, but may not as serine and threonine are both polar, uncharged amino acids.

Nine different FLRFamide-like peptides were queried using input sequences from *H. americanus* in the brain and STG transcriptomes of *L. emarginata* and *P. producta,* and in the brain and eyestalk transcriptomes of *C. opilio*. No hits were obtained for any of these peptides. This was an unexpected result as these peptides have been observed in other decapod crustaceans including *H. americanus* (Christie et al., 2017). However, given the very short query sequences it is very likely that they did not pass the statistical significance threshold set by the BLAST

protocol. In order to determine the existence of FMRFamide-like peptide sequences, the transcriptomes were translated into peptide sequences by longest open reading frame through TransDecoder and then searched directly, bypassing BLAST statistics, for FLRFG containing peptide sequences. We found six active peptide regions that contained either FLRFG sequences or the similar YLRFG sequence. One of these sequences, NRNFLRFG, was identical to a FMRFamide-like peptide deduced from the eyestalk transcriptome of *H. americanus* (Christie et al., 2017). The inexistence of more identical FMRFamide-like peptide sequences is indicative of the high interspecies variability of these peptides, which may pose a challenge in their application to physiological preparations.

Sequences from the FLRFamide family peptide myosuppressin were found in the brains of both *L. emarginata* and *P. producta,* as well as in both *C. opilio* transcriptomes. Physiologically, myosuppressin was found to modulate the pyloric pattern in *C. opilio* and has been previously shown to modulate the pyloric pattern in both *P. producta* and *L. emarginata* (Miller, 2018). These findings suggest that myosuppressin receptors exist in the STG of these crab species. Given sequence homology of the active peptide region with *H. americanus*, it is likely that the myosuppressin receptor in these three crab species is similar to the homologous receptor in *H. americanus.*

Prepro-RPCH sequences were found in the brain of *L. emarginata* but not in the STG, nor in the STG of *P. producta.* Even though RPCH was shown to modulate the pyloric pattern of *L. emarginata*, it is important to note that RPCH is synthesized in the oesophageal and commissural ganglia and secreted into the STG via anterior projections. Therefore, the transcription of RPCH does not occur in the STG. In *stn*-intact preparations of *P. producta*, RPCH does not modulate the pyloric pattern (Dickinson et al., 2008). However, since RPCH has

many other roles in other *P. producta* organs, we expected to see transcripts in the brain. Additionally, mass spectrometric analysis reveals ion peaks corresponding to RPCH in the sinus glands and STNS of *P. producta*, verifying its presence (Dickinson et al., 2008). Prepro-RPCH peptide sequences were found in both *C. opilio* transcriptomes.

Conclusions

In conclusion, the pyloric patterns of *C. opilio* and *L. emarginata* appear to be modulated by all seven neuromodulators tested in this study, while *P. producta* shows a much narrower modulatory capacity. Although the effects of modulators on the STNS of *C. opilio* were not significant, we can qualitatively determine that these seven neuromodulators impacted the pyloric pattern. This supports the hypothesis that neuromodulation is a substrate for behavioral evolution, in this case diet diversity.

Future study will focus on expanding the sample size of *C. opilio* STNS preparations and adding other neuromodulators to be tested. One potential class of signaling peptides to examine are the CCHamide and diuretic hormone families. Additionally, Liquid Chromatography Mass Spectrometry (LCMS) should be performed through previously described methods to verify the existence of the neuromodulators in *C. opilio* and which secretory tissues they may originate from (Dickinson et al., 2008; Ma et al., 2008).

Through next-generation sequencing and *de novo* transcriptomics, we have assembled tissue-specific transcriptomes for these three members of the Majoidea super family. In order to understand the mechanism by which neuromodulatory capacity is able to differ interspecifically, continued mining of the transcriptomes for the Majoidea superfamily is necessary. In addition to exploratory analysis of modulator sequences, these transcriptomes must be mined for the

receptors of these modulators. qPCR analysis can then be performed to determine the relative expression levels of these receptors in the STNS between species.

REFERENCES

Almagro Armenteros JJ, Tsirigos KD, Sonderby CK, Petersen TN, Winther O, Brunak S, von Heijne G, and Nielsen H. SignalP 5.0 improves signal peptide predictions using deep neural networks. *Nat Biotechnol* 37: 420-423, 2019.

Artimo P, Jonnalagedda M, Arnold K, Baratin D, Csardi G, de Castro E, Duvaud S, Flegel V, Fortier A, Gasteiger E, Grosdidier A, Hernandez C, Ioannidis V, Kuznetsov D, Liechti R, Moretti S, Mostaguir K, Redaschi N, Rossier G, Xenarios I, and Stockinger H. ExPASy: SIB bioinformatics resource portal. *Nucleic Acids Res* 40: W597-603, 2012.

Blitz DM, White RS, Saideman SR, Cook A, Christie AE, Nadim F, and Nusbaum MP. A newly identified extrinsic input triggers a distinct gastric mill rhythm via activation of modulatory projection neurons. *J Exp Biol* 211: 1000-1011, 2008.

Bolger AM, Lohse M, and Usadel B. Trimmomatic: a flexible trimmer for Illumina sequence data. *Bioinformatics* 30: 2114-2120, 2014.

Cerveau N, and Jackson DJ. Combining independent de novo assemblies optimizes the coding transcriptome for nonconventional model eukaryotic organisms. *BMC Bioinformatics* 17: 525, 2016.

Christie A, Lundquist C, Nässel D, and Nusbaum M. Two novel tachykinin-related peptides from the nervous system of the crab Cancer borealis. *Journal of Experimental Biology* 200: 2279-2294, 1997.

Christie A, Skiebe P, and Marder E. Matrix of neuromodulators in neurosecretory structures of the crab Cancer borealis. *Journal of Experimental Biology* 198: 2431-2439, 1995.

Christie AE, Roncalli V, Cieslak MC, Pascual MG, Yu A, Lameyer TJ, Stanhope ME, and Dickinson PS. Prediction of a neuropeptidome for the eyestalk ganglia of the lobsterHomarus americanususing a tissue-specificde novoassembledtranscriptome. *General and Comparative Endocrinology* 243: 96-119, 2017.

Daur N, Nadim F, and Bucher D. The complexity of small circuits: the stomatogastric nervous system. *Current Opinion in Neurobiology* 41: 1-7, 2016.

Dickinson PS. Neuromodulation of central pattern generators in invertebrates and vertebrates. *Curr Opin Neurobiol* 16: 604-614, 2006.

Dickinson PS, and Nagy F. Control of a central pattern generator by an identified modulatory interneurone in crustacea. II. Induction and modification of plateau properties in pyloric neurones. *J Exp Biol* 105: 59-82, 1983.

Dickinson PS, Stemmler EA, and Christie AE. The pyloric neural circuit of the herbivorous crab Pugettia producta shows limited sensitivity to several neuromodulators that elicit robust effects in more opportunistically feeding decapods. *J Exp Biol* 211: 1434-1447, 2008.

Fu L, Niu B, Zhu Z, Wu S, and Li W. CD-HIT: accelerated for clustering the next-generation sequencing data. *Bioinformatics* 28: 3150-3152, 2012.

Govind CK, and Lingle CJ. Neuromuscular Organization and Pharmacology. In: *The Crustacean Stomatogastric System: A Model for the Study of Central Nervous Systems*, edited by Selverston AI, and Moulins M. Berlin Heidelberg: Springer-Verlag, 1987.

Grabherr M, Haas B, Yassour M, Levin J, Thompson D, Amit I, Adiconis X, Fan L, Raychowdhury R, Zeng Q, Chen Z, Mauceli E, Hacohen N, Gnirke A, Rhind N, di Palma F, Birren BW, Nusbaum C, Lindblad-Toh K, Friedman N, and Regev A. Full-length transcriptome assembly from RNA-Seq data without a reference genome. *Nature Biotechnology* 29: 644-652, 2011.

Haas BJ, Papanicolaou A, Yassour M, Grabherr M, Blood PD, Bowden J, Couger MB, Eccles D, Li B, Lieber M, MacManes MD, Ott M, Orvis J, Pochet N, Strozzi F, Weeks N, Westerman R, William T, Dewey CN, Henschel R, LeDuc RD, Friedman N, and Regev A. De novo transcript sequence reconstruction from RNA-seq using the Trinity platform for reference generation and analysis. *Nat Protoc* 8: 1494-1512, 2013.

Harris-Warrick R. Mechanisms for neuromodulation of biological neural networks. In: *Advances in Neural Information Processing Systems 2*, edited by Touretzky DNeural Information Processing Systems Foundation, 1989, p. 18-27.

Harris-Warrick R, Nagy F, and Nusbaum M. Neuromodulation of stomatogastric networks by identified neurons and transmitters. In: *Dynamic Biological Networks: The Stomatogastric Nervous System*, edited by Harris-Warrick R, Marder E, Selverston AI, and Moulins M. Cambridge, MA: MIT Press, 1992, p. 87-138.

Hooper S, and Marder E. Modulation of the lobster pyloric rythm by the peptide proctolin. *Journal of Neuroscience* 7: 2097-2112, 1987.

Hoover BA, Nguyen H, Thompson L, and Wright WG. Associative memory in three aplysiids: correlation with heterosynaptic modulation. *Learn Mem* 13: 820-826, 2006.

Hui L, Zhang Y, Wang J, Cook A, Ye H, Nusbaum MP, and Li L. Discovery and functional study of a novel crustacean tachykinin neuropeptide. *ACS Chem Neurosci* 2: 711-722, 2011.

Hultgren KM, and Stachowicz JJ. Molecular phylogeny of the brachyuran crab superfamily Majoidea indicates close congruence with trees based on larval morphology. *Mol Phylogenet Evol* 48: 986-996, 2008.

Kadiri LR, Kwan AC, Webb WW, and Harris-Warrick RM. Dopamine-induced oscillations of the pyloric pacemaker neuron rely on release of calcium from intracellular stores. *J Neurophysiol* 106: 1288-1298, 2011.

Katz PS, and Harris-Warrick RM. The evolution of neuronal circuits underlying species-specific behavior. *Curr Opin Neurobiol* 9: 628-633, 1999.

Langmead B, and Salzberg SL. Fast gapped-read alignment with Bowtie 2. *Nat Methods* 9: 357-359, 2012.

Li H, Handsaker B, Wysoker A, Fennell T, Ruan J, Homer N, Marth G, Abecasis G, Durbin R, and Genome Project Data Processing S. The Sequence Alignment/Map format and SAMtools. *Bioinformatics* 25: 2078-2079, 2009.

Ma M, Chen R, Sousa GL, Bors EK, Kwiatkowski MA, Goiney CC, Goy MF, Christie AE, and Li L. Mass spectral characterization of peptide transmitters/hormones in the nervous system and neuroendocrine organs of the American lobster Homarus americanus. *Gen Comp Endocrinol* 156: 395-409, 2008.

Marder E, and Bucher D. Central pattern generators and the control of rhythmic movements. *Curr Biol* 11: R986-996, 2001.

Marder E, and Bucher D. Understanding Circuit Dynamics Using the Stomatogastric Nervous System of Lobsters and Crabs. *Annual Review of Physiology* 69: 291-316, 2007.

Marder E, and Eisen JS. Electrically coupled pacemaker neurons respond differently to same physiological inputs and neurotransmitters. *J Neurophysiol* 51: 1362-1374, 1984.

Maynard DM, and Dando MR. The structure of the stomatogastric neuromuscular system in Callinectes isapdu, Homarus americanus and Panulirus argus (Decapoda Crustacea). *Philosophical Transactions of The Royal Society of London* 268: 171-220, 1974.

Miller AI. Does a central pattern generating system's modulatory ability underlie its behavioral diversity? In: *Neuroscience*. Brunswick, Maine: Bowdoin College, 2018.

Norris BJ, Coleman MJ, and Nusbaum MP. Recruitment of a projection neuron determines gastric mill motor pattern selection in the stomatogastric nervous system of the crab, Cancer borealis. *J Neurophysiol* 72: 1451-1463, 1994.

Northcutt AJ, Kick DR, Otopalik AG, Goetz BM, Harris RM, Santin JM, Hofmann HA, Mader E, and Schulz DJ. Molecular profiling of single neurons of known identity in two ganglia from the crab Cancer borealis. *Proceedings of the National Academy of Sciences* 116: 26980-26990, 2019.

Nusbaum M, and Marder E. A Neuronal Role For a Crustacean Red Pigment Concentrating Hormone-Like Peptide: Neuromodulation of the Pyloric Rhythm in the Crab, Cancer Borealis. *Journal of Experimental Biology* 135: 165-181, 1988.

Nusbaum MP, and Marder E. A modulatory proctolin-containing neuron (MPN). II. State-dependent modulation of rhythmic motor activity. *The Journal of Neuroscience* 9: 1600-1607, 1989.

Peck JH, Gaier E, Stevens E, Repicky S, and Harris-Warrick RM. Amine modulation of Ih in a small neural network. *J Neurophysiol* 96: 2931-2940, 2006.

Perkins EB, and Snook T. Control of Pigment Migration in the Chromatophores of Crustaceans. *Proc Natl Acad Sci U S A* 17: 282-285, 1931.

R Core Team. R: a language and environment for statistical computing. Vienna, Austria: R Foundation for Statistical Computing, 2017.

Sainte-Marie B, Sévigny J, and Gauthier Y. Laboratory behavior of adolescent and adult males of the snow crab (Chionoecetes opilio) (Brachyura: Majidae) mated noncompetitively and competitively with primiparous females. *Candian Journal of Fisheries and Aquatic Science* 54: 239-248, 1997.

Selverston AI, Szucs A, Huerta R, Pinto R, and Reyes M. Neural mechanisms underlying the generation of the lobster gastric mill motor pattern. *Front Neural Circuits* 3: 12, 2009.

Seppey M, Manni M, and Zdobnov EM. BUSCO: Assessing Genome Assembly and Annotation Completeness. *Methods Mol Biol* 1962: 227-245, 2019.

Stavrianakou M, Perez R, Wu C, Sachs MS, Aramayo R, and Harlow M. Draft de novo transcriptome assembly and proteome characterization of the electric lobe of Tetronarce californica: a molecular tool for the study of cholinergic neurotransmission in the electric organ. *BMC Genomics* 18: 611, 2017.

Stemmler EA, Gardner NP, Guiney ME, Bruns EA, and Dickinson PS. The detection of red pigment-concentrating hormone (RPCH) in crustacean eyestalk tissues using matrix-assisted laser desorption/ionization-Fourier transform mass spectrometry: [M + Na]+ ion formation in dried droplet tissue preparations. *J Mass Spectrom* 41: 295-311, 2006.

Thorvaldsdottir H, Robinson JT, and Mesirov JP. Integrative Genomics Viewer (IGV): high-performance genomics data visualization and exploration. *Brief Bioinform* 14: 178-192, 2013.

Thurmond J, Goodman JL, Strelets VB, Attrill H, Gramates LS, Marygold SJ, Matthews BB, Millburn G, Antonazzo G, Trovisco V, Kaufman TC, Calvi BR, and FlyBase C. FlyBase 2.0: the next generation. *Nucleic Acids Res* 47: D759-D765, 2019.

Turrigiano GG, and Selverston AI. Cholecystokinin-like peptide is a modulator of a crustacean central pattern generator. *Journal of Neuroscience* 9: 2486-2501, 1989.

Vanderveken M, and O'Donnell MJ. Effects of diuretic hormone 31, drosokinin, and allatostatin A on transepithelial K(+) transport and contraction frequency in the midgut and hindgut of larval Drosophila melanogaster. *Arch Insect Biochem Physiol* 85: 76-93, 2014.

Veenstra JA. Mono- and dibasic proteolytic cleavage sites in insect neuroendocrine peptide precursors. *Archives of Insect Biochemistry and Physiology* 43: 49-63, 2000.

Waterhouse RM, Seppey M, Simao FA, Manni M, Ioannidis P, Klioutchnikov G, Kriventseva EV, and Zdobnov EM. BUSCO Applications from Quality Assessments to Gene Prediction and Phylogenomics. *Mol Biol Evol* 35: 543-548, 2018.

Weimann JM, Skiebe P, Heinzel HG, Soto C, Kopell N, Jorge-Rivera JC, and Marder E. Modulation of oscillator interactions in the crab stomatogastric ganglion by crustacean cardioactive peptide. *J Neurosci* 17: 1748-1760, 1997.

Wickham H. *ggplot2: Elegant Graphics for Data Analysis*. New York: Springer-Verlag, 2016.

Appendix: Input prepro-peptide sequences

Prepro-proctolin from *H. americanus* (Christie et al., 2017)
MTRTGLVVVVALVVLAAALTQARYLPTRADDTRLDEIRELLREMLERTAEGANSRISGSGYDKR
FMYKRSVPEEGAAEMVQPALNLPQ

Prepro-crustacean cardioactive peptide (CCAP) from *D. melanogaster* (Thurmond et al., 2019)
MRTSMRISLRLLALLACAICSQASLERENNEGTNMANHKLSGVIQWKYEKRPFCNAFTGCGRKR
TYPSYPPFSLFKRNEVEEKPYNNEYLSEGLSDLIDINAEPAVENVQKQIMSQAKIFEAIKEASK
EIFRQKNKQKMLQNEKEMQQLEERESK

Prepro-red pigment concentrating hormone (RPCH) from *H. americanus (*Christie et al., 2017)
MVRAGCALMLVVVVFASCVSAQLNFSPGWGKRAAAASGTDPAAASLHPAPPAVLTAASGANAGD
SCGTIPVSAVMHIYRLIRTEAARLIQCQEEYMG

Prepro-diuretic hormone 31 (DH31) from *H. americanus (*Christie et al., 2017)
MNSTGAVFVSLVVAFIFVSSVNSAAFNREARAVVQIEDPDYVLELLTRLGHSIIRANELEKFVR
SSGSAKRGLDLGLGRGFSGSQAAKHLMGLAAANFAGGPGRRRRSSDDGLDLHHDDNLYAQDQAA
DLAESSR

Prepro-myosuppressin from *H. americanus* (Christie et al., 2017)
MVFRSCSWSCLLVVGVVVVMGVCVGVGETMPPPICLSQQVPLSPFAKKLCSALINISEFSRAME
EYLGAQAIERSMPVNEPEVKRQDLDHVFLRFGRSQQ

Prepro-CCHamide I from *H. americanus* (Christie et al., 2017)
MSRGMINVFLVVLGVVALSSQAWGSCSQFGHSCFGAHGKRDGDQYARQEPSPLYOEANQLPEFE
QRQEDRLSVDEAVTDREIVANARNWLAVLSHRLRQRTSPQSSPSAQSLGYFQ